KEK-TH-1567

Vacuum birefringence in strong magnetic fields: (I) Photon polarization tensor with all the Landau levels

Koichi Hattori*

Theory Center, IPNS, High energy accelerator research organization (KEK), 1-1 Oho, Tsukuba, Ibaraki 305-0801, Japan and Institute of Physics and Applied Physics, Yonsei University, Seoul 120-749, Korea [b]

Kazunori Itakura‡

Theory Center, IPNS, High energy accelerator research organization (KEK), 1-1 Oho, Tsukuba, Ibaraki 305-0801, Japan and Department of Particle and Nuclear Studies, Graduate University for Advanced Studies (SOKENDAI), 1-1 Oho, Tsukuba, Ibaraki 305-0801, Japan

Abstract

Photons propagating in strong magnetic fields are subject to a phenomenon called the "vacuum birefringence" where refractive indices of two physical modes both deviate from unity and are different from each other. We compute the vacuum polarization tensor of a photon in a static and homogeneous magnetic field by utilizing Schwinger's proper-time method, and obtain a series representation as a result of double integrals *analytically* performed with respect to proper-time variables. The outcome is expressed in terms of an infinite sum of known functions which is plausibly interpreted as summation over all the Landau levels of fermions. Each contribution from infinitely many Landau levels yields a kinematical condition above which the contribution has an imaginary part. This indicates decay of a sufficiently energetic photon into a fermion-antifermion pair with corresponding Landau level indices. Since we do not resort to any approximation, our result is applicable to the calculation of refractive indices in the whole kinematical region of a photon momentum and in any magnitude of the external magnetic field.

[b] current address

* khattori@post.kek.jp

‡ kazunori.itakura@kek.jp

I. INTRODUCTION

It has been long studied that structure of the quantum vacuum in QED would be modified in the presence of externally applied strong electromagnetic fields [1, 2], and modification of the vacuum could entail novel phenomena such as vacuum birefringence of a photon, photon decay into an electron-positron pair, and photon splitting. It is natural to expect these effects to occur because the vacuum in QED is filled with electrons in the Dirac sea, and they react as 'media' like in ordinary substances in response to external fields [3]. Whereas any such effect has not been established in experiments, recent years have witnessed an increasing interest in possibilities that extremely strong electromagnetic fields would be realized in several different situations (see, for example, Ref. [4] for a wide range of physics related to strong fields). Primary examples are relativistic (non-central) heavy-ion collisions [5–8] and strongly-magnetized compact stars such as magnetars [9], both of which are thought to accompany electromagnetic fields far stronger than so-called the "critical field" for electrons,[1] $B_c = E_c \equiv m_e^2/|e|$. Many observable effects are proposed in relation to magnetars [10] and also to heavy-ion collisions [8, 11, 12]. Besides, intensity of high-field laser has been rapidly increasing and is now about to reach the critical field strength. Many authors have been addressing theoretical aspects of the possible vacuum physics that could be studied by the ultra-high-intensity laser (see for example, Ref. [13]). Thus, in near future, we would be able to study the vacuum physics in strong fields in somewhat controllable environments. With these current situations in mind, we should further pursue towards deeper understanding of the vacuum physics in strong fields.

In the present paper, we provide a theoretical framework necessary for the description of vacuum birefringence and photon decay in strong magnetic fields which are typical and important examples of the vacuum physics in strong fields. We give an *analytic* expression for the vacuum polarization tensor of a photon within one loop of a 'dressed' fermion that includes all-order interaction with the external field at tree level. Notice that the strong fields compensate the smallness of the coupling constant, making a particular kind of higher-order diagrams enhanced. Moreover, when the fields are stronger than the critical ones, naïve perturbative expansion breaks down and thus one has to sum up all-order diagrams that are

[1] Since the magnetic axis of a magnetar is generally not the same as the rotation axis (thus, a pulsar), the magnetic field shows strong time dependence and will induce an electric field of the similar order of strength.

enhanced by the external fields. The dressed fermion propagator which appears in the one-loop diagram is obtained after such resummation with respect to the external fields. As a result of resummation of higher-order diagrams, observables acquire nonlinear dependences on the external field. Since interaction with the external field is encoded as a linear coupling at the Lagrangian level, strong-field physics describing this kind of nonlinear effect is called the "nonlinear QED".

In spite of a simple structure of the one-loop diagram, complete description of the vacuum polarization tensor in the whole kinematical region has not been available so far. While the vacuum polarization tensor at the one-loop level is given in an integral representation with respect to two proper-time variables [14–17, 19–21], its integrand is composed of rapidly oscillating exponential factors which have prevented previous studies from precise analytic and even numerical understanding of the phenomena. Because of this difficulty, our understanding of the vacuum birefringence was limited to a restricted phase space of the photon momentum [16–18] or to a strong-filed case where lowest Landau level approximation is applicable [19]. We show however that the double proper-time integral can be analytically performed owing to a double infinite series expansions of the integrand. Since our calculation does not resort to any approximation, the result is applicable to any value of a photon momentum and any magnitude of the external field. Namely, our result can also treat, as well as the vacuum birefringence, the photon decay into a fermion-antifermion pair which occurs when the photon energy is sufficiently large.

This paper is organized as follows. First, in Sec. II, we present the integral representation of the vacuum polarization tensor of a photon in the external magnetic field. Then, in Sec. III, we explain how the vacuum birefringence appears in strong magnetic fields. Analytic evaluation of the integral is discussed in detail in Sec. IV. In this section, we also provide physical interpretation of the double infinite series expansion, and then carefully investigate singularity structure of the vacuum polarization tensor. Kinematical condition of the photon decay also appears here. Summary and prospects are given in the last section where we mention another important step to obtain the refractive indices. In Appendices, we explain supplemental materials such as details of the proper-time method, renormalization issues, and so on. In principle, we are able to calculate the refractive indices by using the polarization tensor obtained in the present paper. Taking care of the procedure mentioned in the last section, we will show the results of refractive indices in the next paper [22].

II. VACUUM POLARIZATION TENSOR IN EXTERNAL FIELDS

In this section, we provide theoretical framework for the vacuum polarization tensor of a propagating photon in a strong external field, which is necessary for the calculation of the refractive indices. In particular, we discuss the case of a strong *magnetic* field, but the techniques developed in this section should be equally applied to a case with a strong *electric* field, which will be reported separately.

We consider a system of massive charged fermions interacting with photons. Thus we start with the standard spinor QED Lagrangian:

$$\mathscr{L} = \bar{\psi}\left(i\not{D} - m\right)\psi - \frac{1}{4}F^{\mu\nu}F_{\mu\nu} \ , \tag{1}$$

where we adopt a convention for the covariant derivative, $D^\mu = \partial^\mu + ieA^\mu(x)$ [23]. Here, "e" and "m" representatively denote charge and mass of a fermion (e is negative for an electron). Since the gauge field A^μ contains both the external field $A^\mu_{\rm cl}$ and dynamical (i.e., propagating) degrees of freedom a^μ: $A^\mu = A^\mu_{\rm cl} + a^\mu$, the fermion kinetic term in the Lagrangian (1) determines the coupling of the fermion to the external field. Whereas the fundamental QED Lagrangian (1) describes only the linear interaction at the classical level, some of higher-order quantum effects become important when they are enhanced due to the strong external field, and give rise to nonlinear interaction among photons. For example, when the external field is a strong magnetic field, insertion of an external field line gives a factor of $\mathcal{O}(|eB|/m^2)$ and n external field lines, $\mathcal{O}((|eB|/m^2)^n)$, thereby one has to sum up all the diagrams when B is larger than the critical field $B \gtrsim B_c \equiv m^2/|e|$ to obtain a "dressed" fermion propagator. This effect is shown in Fig. 1. Since this dressed fermion propagator includes all-order contributions with respect to eB, any process involving the dressed fermions becomes nonlinear with respect to the external field B, and nonperturbative. Similarly, one can define the critical electric field $E_c \equiv m^2/|e|$ which also indicates breakdown of the ordinary perturbative expansion. However, electric fields beyond E_c induce instability of the vacuum [2, 24], called the Schwinger mechanism, and will be screened by creation of fermion-antifermion pairs. On the other hand, the critical magnetic field B_c just indicates onset of strong nonlinear effects, and it makes sense to treat magnetic fields stronger than the critical one. Thus, as far as one considers static magnetic fields, one can discuss very strong nonlinear regime in QED. This is called the "nonlinear QED" regime.

If there are several species of fermions $\psi^{(i)}$ with different masses $m_{(i)}$ and charges $e_{(i)}$, one can define critical magnetic fields $B_c^{(i)} = m_{(i)}^2/|e_{(i)}|$ corresponding to each fermion: $B_c^{(1)} < B_c^{(2)} < \cdots$. Since magnetic fields can become stronger than the (minimum) critical field (unlike the critical electric field beyond which the Schwinger mechanism occurs), one has to include all the relevant fermion degrees of freedom when one treats very strong magnetic field; typically if $B_c^{(n)} < B < B_c^{(n+1)}$, then at least we need to include fermions up to $\psi^{(n)}$. In the present paper, however, we provide formula only with the lightest fermion. Contributions of heavier fermions are easily obtained by appropriate replacements of the electric charge and the mass by those of the heavier fermions. Note also that contributions from different fermions are all additive in the vacuum polarization tensor.

A fundamental key ingredient is the fermion propagator in an external field $G(x, y|A_{\rm cl}) \equiv \langle 0|T\psi(x)\bar{\psi}(y)|0\rangle$ which includes all the interactions with the external field. Recall that the propagator is a Green's function of the Dirac operator. If one includes only the external field into the Dirac operator, the propagator satisfies (in the momentum space),

$$\left(\not{p} - e\not{A}_{\rm cl} - m\right) G(p|A_{\rm cl}) = i\,. \tag{2}$$

Therefore, one finds

$$G(p|A_{\rm cl}) = \frac{i}{\not{p} - e\not{A}_{\rm cl} - m} \tag{3}$$

$$= \frac{i}{\not{p} - m} \sum_{n=0}^{\infty} \left[\ (-ie\not{A}_{\rm cl}) \frac{i}{\not{p} - m}\ \right]^n . \tag{4}$$

The last expression allows us to diagrammatically depict the nonlinear interaction with the external field as shown in Fig. 1.

When one considers the propagation of a photon in a strong background field $A_{\rm cl}^\mu$, one uses the fermion propagator (3). For example, a one-loop contribution of a photon self-energy is computed as in Fig. 2. Thus, modification of the fermion propagator due to the external field causes a significant influence on the photon propagation. Representing the photon self-energy, or equivalently the vacuum polarization tensor, in a constant external field as $\Pi_{\rm ex}^{\mu\nu}(x-y)$, one finds that the kinetic term of the propagating mode a^μ acquires a quantum effect as, $\mathscr{L}_A^{\rm loop} = \frac{1}{2}\int dy\ a_\mu(x)\ \Pi_{\rm ex}^{\mu\nu}(x-y)\ a_\nu(y)$. Then, the Euler-Lagrange equation for a^μ leads to a modified Maxwell equation, $[\ q^2\eta^{\mu\nu} - q^\mu q^\nu - \Pi_{\rm ex}^{\mu\nu}(q)\ ]\, a_\nu(q) = 0$. Although the vacuum polarization in the ordinary vacuum does not modify photon propagation owing

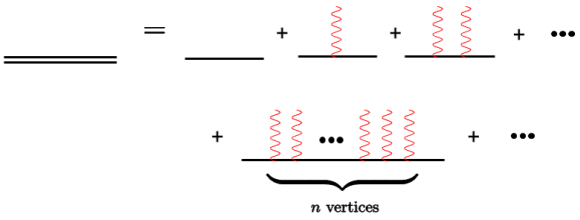

FIG. 1. Dressed fermion propagator (a double line) includes all the tree-level interactions with a strong external field (wavy lines).

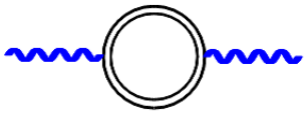

FIG. 2. One-loop diagram of the vacuum polarization tensor in a strong magnetic field.

to the gauge and Lorentz symmetries, we show that quantum excitations in an externally applied electromagnetic field behave like electron-hole excitations in dielectric substances [3]. Indeed, the vacuum polarization tensor corresponds to a response function of the Dirac sea to an electromagnetic field induced by an incident photon.

To compute the vacuum polarization tensor in the external field, we use the "proper-time method" which was developed by J. Schwinger [24]. One can equivalently rewrite the dressed propagator (3) in a different way as

$$G(p|A_{\rm cl}) = i\left(\not{p} - e\not{A}_{\rm cl} + m\right) \times \frac{1}{i}\int_0^\infty d\hat{\tau}\ \mathrm{e}^{i\hat{\tau}\left\{(\not{p}-e\not{A}_{\rm cl})^2-(m^2-i\varepsilon)\right\}}\,, \tag{5}$$

where the integral with respect to the "proper time" $\hat{\tau}$ is convergent owing to a prescription by $-i\varepsilon$. Note that $\hat{\tau}$ has dimension of inverse mass squared. Infinite sum with respect to the external field is now encoded into the exponential factor in the integrand. As summarized in Appendix A, one can explicitly compute $G(p|A_{\rm cl})$ when the external field is constant.

By using the dressed propagator shown in Eq. (A7), we can now calculate the 1-loop vacuum polarization tensor in the external magnetic field (see Fig. 2):

$$i\,\Pi^{\mu\nu}_{\rm ex}(q) = (-ie)^2(-1)\int\frac{d^4p}{(2\pi)^4}\mathrm{Tr}\Big[\ \gamma^\mu G(p|A_{\rm cl})\gamma^\nu G(p+q|A_{\rm cl})\ \Big]\,, \tag{6}$$

where an overall minus sign arises from the fermion loop. This is a gauge invariant quantity and should be independent of the gauge we adopt.[2] Note that momentum integration gives rise to an ultraviolet divergence, because the fermion propagator behaves as $G(p|A_{\rm cl}) \sim p^{-1}$ for large p. While we find a quadratic superficial degree of divergence from a naïve power

[2] In the actual calculation, however, we adopt specific gauges. For computation of the fermion propagator $G(p|A_{\rm cl})$, we worked in the Fock-Schwinger gauge for the background field $A_{\rm cl}$ (see Appendix A). As we will see below, we then compute the polarization tensor in the covariant gauge which fixes the residual gauge symmetry of the dynamical gauge field a^μ.

counting, it actually diverges logarithmically owing to a specific tensor structure demanded by the Ward identity, $q_\mu \Pi^{\mu\nu}_{\rm ex}(q) = 0$. We will explicitly show a gauge invariant form of the vacuum polarization tensor in the following, and comment on renormalization in the end of this section.

It has been known that the vacuum polarization tensor is endowed with a gauge-invariant tensor structure in terms of three transverse-projection operators satisfying $q_\mu P_i^{\mu\nu} = 0$. Their explicit forms are given by

$$\Pi^{\mu\nu}_{\rm ex}(q) = -\Big(\chi_0 P_0^{\mu\nu} + \chi_1 P_1^{\mu\nu} + \chi_2 P_2^{\mu\nu}\Big)\,, \tag{7}$$

$$P_0^{\mu\nu} = q^2\eta^{\mu\nu} - q^\mu q^\nu\ , \quad P_1^{\mu\nu} = q_\parallel^2 \eta_\parallel^{\mu\nu} - q_\parallel^\mu q_\parallel^\nu\ , \quad P_2^{\mu\nu} = q_\perp^2 \eta_\perp^{\mu\nu} - q_\perp^\mu q_\perp^\nu\,, \tag{8}$$

where we suppressed arguments of Lorentz-scalar functions χ_i $(i = 0, 1, 2)$, of which explicit expressions are immediately shown below. We now apply the external magnetic field along the third axis of spatial coordinates in the negative direction so that $eB^3 > 0$ for an electron (B^3 is the third component of the magnetic field vector B^i). Since the presence of the magnetic field specifies a preferred direction, one distinguishes longitudinal and transverse directions with respect to the magnetic field. The metric tensor $\eta^{\mu\nu} = {\rm diag}(1, -1, -1, -1)$ is decomposed into longitudinal and transverse subspaces $\eta_\parallel^{\mu\nu} = {\rm diag}(1, 0, 0, -1)$ and $\eta_\perp^{\mu\nu} = {\rm diag}(0, -1, -1, 0)$, respectively. Similarly, longitudinal and transverse momenta are defined as $q_\parallel^\mu = (q^0, 0, 0, q^3)$ and $q_\perp^\mu = (0, q^1, q^2, 0)$, respectively.

In the proper-time method (see Appendix A for more details), the polarization tensor (6) has integrals with respect to the momentum p, and two proper times which we denote $\hat\tau_1$ and $\hat\tau_2$ corresponding to each propagator (see Eq. (5)). The integration over p is just a Gaussian integral, and can be straightforwardly performed. Then, we rewrite the remaining integrals by using two dimensionless variables $\tau = eB(\hat\tau_1 + \hat\tau_2)/2$ and $\beta = eB(\hat\tau_1 - \hat\tau_2)/\tau$. Notice that the scalar functions χ_i $(i = 0, 1, 2)$ are dimensionless, and thus we further introduce three dimensionless variables, $B_{\rm r} = B/B_c$, $r_\parallel^2 = \frac{q_\parallel^2}{4m^2}$ and $r_\perp^2 = \frac{q_\perp^2}{4m^2} = -\frac{|\boldsymbol{q}_\perp|^2}{4m^2}$ so that the scalar functions χ_i are expressed as

$$\chi_i(r_\parallel^2, r_\perp^2; B_{\rm r}) = \frac{\alpha}{4\pi}\int_{-1}^{1} d\beta \int_0^\infty d\tau\ \frac{\Gamma_i(\tau,\beta)}{\sin\tau}\ {\rm e}^{-iu\cos(\beta\tau)}\ {\rm e}^{i\eta\cot\tau}\ {\rm e}^{-i\phi_\parallel \tau}\,, \tag{9}$$

where we have introduced two shorthand notations: $\eta \equiv -2r_\perp^2/B_{\rm r}$ and $u \equiv \eta/\sin\tau$, and lastly $\phi_\parallel$ and Γ_i are known functions given by the following [14–17, 19] (see also Refs. [20, 21]

for details):

$$\phi_{\parallel}(r_{\parallel}^2, B_{\rm r}) = \frac{1}{B_{\rm r}} \left\{ \, 1 - (1-\beta^2) \, r_{\parallel}^2 \, \right\} , \tag{10}$$

and

$$\begin{aligned} \Gamma_0(\tau,\beta) &= \cos(\beta\tau) - \beta \sin(\beta\tau) \cot\tau \, , \\ \Gamma_1(\tau,\beta) &= (1-\beta^2)\cos\tau - \Gamma_0(\tau,\beta) \, , \\ \Gamma_2(\tau,\beta) &= 2\frac{\cos(\beta\tau)-\cos\tau}{\sin^2\tau} - \Gamma_0(\tau,\beta) \quad . \end{aligned} \tag{11}$$

In Eq. (9), the coupling constant in the overall factor $\alpha = e^2/4\pi$ comes from propagating photons attached to the fermion one-loop, while the others are from higher-order effects associated with the external magnetic field as is evident from the observation that they always appear with the magnetic field as eB. As will be shown in Sec. IV, the scalar function χ_1 is a real-valued function when $r_{\parallel}^2 \leq 1$, reflecting convergence of the double integral in Eq. (9), and the same holds for the others, χ_0 and χ_2, when $r_{\parallel}^2 \leq (1+\sqrt{1+2B_{\rm r}})^2/4$. Whereas reliable numerical computation has been performed in this kinematical region [18], analytic calculation is necessary for understanding behavior of the polarization tensor in the whole kinematical region. In Sec. IV, we will explicitly perform the remaining two integrals to obtain the analytic expression of the polarization tensor.

We emphasize here that we have neither specified any dispersion relation for the external photon momentum, nor even assumed that the photon is on-shell. We will discuss later that the photon dispersion will be determined as a result of interaction with the external magnetic fields. In general, there will be a deviation from the massless-type dispersion relation indicating that $r_{\parallel}^2 + r_{\perp}^2 \neq 0$ and $\omega \neq |\boldsymbol{q}|$. Accordingly, the longitudinal and transverse momenta appearing in Eqs. (9) – (11) should be treated independently at this moment.

Recall that only χ_0 survives in the ordinary vacuum and is divergent. Divergence of χ_0 is also seen in the presence of the magnetic field (while the others are finite). This can be explicitly verified as follows. First of all, let us see the lower limit of τ integration in Eq. (9). If one takes the limit $\tau \to 0$ in Eq. (11), one finds two of them vanish as $\Gamma_1, \Gamma_2 \to 0$ and thus χ_1 and χ_2 are finite, while χ_0 is logarithmically divergent because $\Gamma_0 \to 1-\beta^2$ as $\tau \to 0$. In other words, subtraction of $\Gamma_0(\tau,\beta)$ in the definition of Γ_1 and Γ_2 ensures the finiteness of χ_1 and χ_2. Next, one can easily identify the origin of the logarithmic divergence by referring the diagrams in Figs. 1 and 2. If one resolves the dressed fermion propagator (a double line) in

Fig. 2 into the sum of external magnetic field insertions as shown in Fig. 1, the first diagram is given by the same vacuum polarization tensor as in the ordinary vacuum without any external field attached. This diagram has a logarithmic divergence as conventionally known. We also notice that this is the only divergent diagram in the series because any additional external leg reduces the degree of divergence. Therefore, the vacuum polarization tensor (9) contains the same divergence as in the ordinary vacuum, without any additional one. As shown in Appendix B in detail, we can remove this logarithmic divergence by adopting an on-shell (with zero transverse momentum) renormalization condition[3] such that a finite vacuum polarization tensor $\hat{\Pi}^{\mu\nu}_{\rm ex}(q_\parallel, q_\perp; B_{\rm r})$ vanishes at the simultaneous limits of on-shell and vanishing field, $r_\parallel^2, r_\perp^2 = 0$ and $B_{\rm r} = 0$. On the basis of this prescription, we define a finite vacuum polarization tensor,

$$\hat{\Pi}^{\mu\nu}_{\rm ex}(q_\parallel, q_\perp; B_{\rm r}) \equiv \Pi^{\mu\nu}_{\rm ex}(q_\parallel, q_\perp; B_{\rm r}) - \Pi^{\mu\nu}_0(0)\,, \tag{12}$$

where the vacuum polarization tensor in the ordinary vacuum $\Pi^{\mu\nu}_0(q^2)$ is obtained in the vanishing field limit as $\lim_{B_{\rm r}\to 0}\Pi^{\mu\nu}_{\rm ex}(q_\parallel, q_\perp; B_{\rm r}) \to \Pi^{\mu\nu}_0(q)$. We will more specifically discuss these things related to renormalization in Appendix B.

III. OPTICAL PROPERTY OF THE VACUUM WITH MAGNETIC FIELDS

Before we go into the detailed calculation of χ_i, let us discuss observable effects of nonzero χ_i, which does not require explicit expressions of χ_i. In particular, we introduce the notions of dielectric constants and refractive indices that are frequently used in context of optics of dielectric substances and semiconductors.

Propagating photons in the ordinary vacuum have two transverse oscillating modes with the dispersion relation of the massless type, $\omega^2 = |\boldsymbol{q}|^2$, which does not vary even if quantum corrections are included, as long as the gauge and Lorentz symmetries are preserved. The presence of an externally applied magnetic field however breaks the Lorentz symmetry, and the dispersion relation of a photon is subject to modification which leads to two intriguing phenomena: Two propagating (physical) modes can have refractive indices different from unity, and a photon is able to decay into a fermion-antifermion pair if its energy is large

[3] Note that the divergence has not been regularized in Eq. (9) – (11). We will introduce appropriate regularizations depending on analytic and numerical calculations, which will be shown in Appendix B.

enough. In this section, we show kinematical aspects of these effects on the basis of the Maxwell equation modified by a nonlinear interaction with the external magnetic field.

In the presence of an external magnetic field, the Maxwell equation for the dynamical photon field a_μ is modified as

$$\left[q^2\eta^{\mu\nu} - \left(1 - \frac{1}{\xi_g}\right) q^\mu q^\nu - \Pi^{\mu\nu}_{\rm ex}(q_\parallel, q_\perp; B_{\rm r}) \right] a_\nu(q) = 0\,, \tag{13}$$

where ξ_g is a parameter in the gauge fixing term, $\mathscr{L}_{\rm GF} = -\frac{1}{2\xi_g}(\partial^\mu a_\mu)^2$. Substituting the vacuum polarization tensor (7), one finds

$$\left[(1+\chi_0)P_0{}^{\mu\nu} + \chi_1 P_1{}^{\mu\nu} + \chi_2 P_2{}^{\mu\nu} + \frac{1}{\xi_g} q^\mu q^\nu \right] a_\nu(q) = 0\,. \tag{14}$$

Below we explain in a qualitative way how the vacuum birefringence and on-shell photon decay follow from this modified Maxwell equation. To this end, explicit expressions of the scalar functions χ_i are not important.

In order to identify two physical modes in the modified Maxwell equation (14), we need to 'diagonalize' the matrix equation by selecting appropriate vectors associated with the direction of the magnetic field. First of all, it should be noticed that one can define three independent vectors that are orthogonal to the momentum of the propagating photon q^μ. In addition to the invariant tensors $\eta^{\mu\nu}$ and $\epsilon^{\mu\nu\rho\sigma}$, one can utilize the field-strength tensor $F^{\mu\nu}$ and the photon momentum q^μ to construct independent vectors. Namely, one finds that the following four vectors $v^\mu_{(\lambda)}$ $(\lambda = 0, \cdots, 3)$ are orthogonal among each other [25]:

$$\begin{aligned} v^\mu_{(0)} &= q^2 F^{\mu\nu}F_{\nu\rho}q^\rho - (q^\nu F_{\nu\rho}F^{\rho\sigma}q^\sigma)q^\mu\,, \\ v^\mu_{(1)} &= F^{\mu\nu}q_\nu\ , \quad v^\mu_{(2)} = \tilde{F}^{\mu\nu}q_\nu\ , \quad v^\mu_{(3)} = q^\mu\,, \end{aligned} \tag{15}$$

where the dual field-strength tensor is defined as $\tilde{F}^{\mu\nu} = \frac{1}{4}\epsilon^{\mu\nu\rho\sigma}F_{\rho\sigma}$ with the completely antisymmetric tensor, $\epsilon^{0123} = 1$. Indeed, one can show the orthogonal relations [4]: $v^\mu_{(\lambda)}\, v_{(\sigma)\mu} = 0$ for any λ and $\sigma(\neq\lambda)$.

Assuming that there is only a magnetic field and it is oriented to the third direction of the spatial coordinates, the set of vectors (15) simplifies to

$$v^\mu_{(0)} = B^2\ (q_\perp^2 q_\parallel^\mu - q_\parallel^2 q_\perp^\mu)\,,$$

[4] In general, when electric ($\boldsymbol{E}$) and magntic ($\boldsymbol{B}$) fields are present, one finds $v^\mu_{(\lambda)}\, v_{(\sigma)\mu} = 0$ except for $v^\mu_{(1)}\, v_{(2)\mu} = -q^2(\boldsymbol{E}\cdot\boldsymbol{B})$. Therefore, the orthogonality among all the vectors holds when $\boldsymbol{E}\cdot\boldsymbol{B} = 0$ and thus $\boldsymbol{E} = 0$ (our case).

$$v^\mu_{(1)} = B\ \tilde{q}^\mu_\perp\ ,\quad v^\mu_{(2)} = B\ \tilde{q}^\mu_\parallel\ ,\quad v^\mu_{(3)} = q^\mu\,, \tag{16}$$

where B is a magnitude of the external magnetic field. For convenience, we have introduced two momentum vectors $\tilde{q}^\mu_\parallel = (q^3, 0, 0, q^0)$ and $\tilde{q}^\mu_\perp = (0, q^2, -q^1, 0)$. They are orthogonal to all the previously introduced momenta, q^μ, $q^\mu_\parallel$ and $q^\mu_\perp$. Therefore, the vectors $\tilde{q}^\mu_\parallel$ and $\tilde{q}^\mu_\perp$ span a space complementary to the space spanned by $q^\mu_\parallel$ and $q^\mu_\perp$.

Notice that the projection operators in the modified Maxwell equation (14) are orthogonal to the momentum vectors, q^μ, $q^\mu_\parallel$ and $q^\mu_\perp$, namely, $q_\mu P_i{}^{\mu\nu} = q_{\parallel\mu} P_i{}^{\mu\nu} = q_{\perp\mu} P_i{}^{\mu\nu} = 0$. This fact suggests that one can represent the projection operators in a different way by using the vectors $\tilde{q}^\mu_\parallel$ and $\tilde{q}^\mu_\perp$. Indeed, two of the projection operators are expressed as $P_1{}^{\mu\nu} = -\tilde{q}^\mu_\parallel \tilde{q}^\nu_\parallel$ and $P_2{}^{\mu\nu} = \tilde{q}^\mu_\perp \tilde{q}^\nu_\perp$. Therefore, one finally finds that the projection operators and thus the modified maxwell equation are 'diagonalized' as follows:

$$P_0{}^{\mu\nu} = q^2\ (\pi^\mu_{(0)}\pi^\nu_{(0)} + \pi^\mu_{(1)}\pi^\nu_{(1)} + \pi^\mu_{(2)}\pi^\nu_{(2)})\ ,\quad P_1{}^{\mu\nu} = q^2_\parallel\ \pi^\mu_{(2)}\pi^\nu_{(2)}\ ,\quad P_2{}^{\mu\nu} = q^2_\perp\ \pi^\mu_{(1)}\pi^\nu_{(1)}\,, \tag{17}$$

$$M^{\mu\nu}(q)a_\nu = \sum_{\lambda=0}^{3} \mathcal{M}_{(\lambda)}(q)\pi^\mu_{(\lambda)}\pi^\nu_{(\lambda)}\, a_\nu = 0\,, \tag{18}$$

where we have rescaled $v^\mu_{(\lambda)}$ so that they have unit norms as[5]

$$\pi^\mu_{(\lambda)} \equiv \frac{v^\mu_{(\lambda)}}{\sqrt{v^\nu_{(\lambda)} v_{(\lambda)\nu}}} \qquad (\lambda = 0, 1, 2, 3)\,. \tag{19}$$

and the coefficients $\mathcal{M}_{(\lambda)}$ are expressed in terms of χ_i. One can easily find the eigen-modes of the modified Maxwell equation by expanding the dynamical photon field in terms of $\pi^\mu_{(\lambda)}$ and assuming a plane wave solution:

$$a^\mu(q) = N \sum_{\lambda=0}^{3} \pi^\mu_{(\lambda)}\ \mathrm{e}^{-i(\omega t - \boldsymbol{q}\cdot\boldsymbol{x})}\quad , \tag{20}$$

where $q^\mu = (\omega, \boldsymbol{q})$ and N is a dimensionful normalization constant. Notice again that we have not specified the dispersion relation which provides a relation between ω and $\boldsymbol{q}$, and this is what we suppose to obtain by solving the modified Maxwell equation. Indeed, one

[5] Our definition of $\pi^\mu_{(\lambda)}$ contains somewhat confusing notation wherein the subscripts of the last two projection operators in Eq. (17) oppositely correspond to those of the vectors on the right-hand sides. However, we keep this notation because the subscripts originally defined in Eq. (15) give natural ordering (i.e., P_1 is given by $\pi_{(1)}$, etc) in case of electric fields.

finds that linear independence of $\pi^\mu_{(\lambda)}$ leads to a set of eigenvalue-equations, [6]

$$\begin{cases} \{\ (1+\chi_0)\ q^2\ \}\ \pi^\mu_{(0)} = 0\,, \\ \{\ (1+\chi_0)\ q^2 + \chi_2\ q_\perp^2\ \}\ \pi^\mu_{(1)} = 0\,, \\ \{\ (1+\chi_0)\ q^2 + \chi_1\ q_\parallel^2\ \}\ \pi^\mu_{(2)} = 0\,, \\ \xi_g^{-1}\ q^2\ \pi^\mu_{(3)} = 0\ \ , \end{cases} \tag{21}$$

which immediately yields the dispersion relation of a photon:

$$\epsilon = \frac{|\boldsymbol{q}|^2}{\omega^2}\,. \tag{22}$$

Here we have defined a dielectric constant ϵ which persists unity in the ordinary vacuum.

It is easily seen that the first and fourth equations lead to dispersion relations of the massless type, $\omega^2 = |\boldsymbol{q}|^2$, with the speed of light in the ordinary vacuum ($\epsilon = 1$), as long as neither $(1+\chi_0) = 0$ nor $\xi_g^{-1} = 0$. However, as explained in Appendix D, these two modes turn out to be unphysical (see Eqs. (D3) and (D4)) and thus we do not discuss them below.

In contrast, the second and third equations yield nontrivial dispersion relations of physical modes. Without loss of generality, we suppose that a photon is propagating in a plane ($y = 0$) spanned by the first and third directions of spatial coordinates, and that the external magnetic field is oriented to the (negative) third direction. The momentum vector q^μ is now represented as $q^\mu = (\omega, |\boldsymbol{q}|\sin(\pi-\theta), 0, |\boldsymbol{q}|\cos(\pi-\theta))$, where θ denotes an angle between the direction of the external magnetic field and the momentum of a propagating photon. Then, the second and third equations yield the vacuum dielectric constants $\epsilon_\perp$ and $\epsilon_\parallel$, respectively:

$$\epsilon_\perp = \frac{1+\chi_0}{1+\chi_0+\chi_2\sin^2\theta} \qquad \text{for} \quad \pi^\mu_{(1)}\,, \tag{23}$$

$$\epsilon_\parallel = \frac{1+\chi_0+\chi_1}{1+\chi_0+\chi_1\cos^2\theta} \qquad \text{for} \quad \pi^\mu_{(2)}\,. \tag{24}$$

The same expressions were obtained in Ref. [19] in the radiation gauge, while we have obtained them in the covariant gauge. The coincidence of two calculations in two different gauges indicates gauge invariance of the dielectric constant, as expected. Whereas we have not specified the explicit form of χ_i, two constants $\epsilon_\perp$ and $\epsilon_\parallel$ are in general not equal to unity and different from each other.[7] Namely, we have found that the externally applied magnetic

[6] We note that the same results can be obtained from the pole position of a photon propagator in the magnetic field (see Appendix C).

[7] In the ordinary vacuum, only χ_0 is nonzero. Even with nonzero χ_0, the above expression reduces to $\epsilon_\perp = \epsilon_\parallel = 1$ when $\chi_1 = \chi_2 = 0$, as expected.

field gives rise to two distinct dielectric constants depending on the polarization directions. This immediately implies that we can define two distinct refractive indices. Therefore, we call this phenomenon *vacuum birefringence* after a similar phenomenon in dielectric substances. Notice also that, due to the violation of the Lorentz symmetry by an external magnetic field, the dielectric constants explicitly depend on the zenith angle with respect to the magnetic field direction. Nevertheless, the system maintains a boost invariance in the direction of the constant external magnetic field, and thus photon propagations in the directions at $\theta = 0, \pi$ are special. Substituting these angles into Eqs. (23) and (24), we find that both of the dielectric constants become unity $\epsilon_\perp(\theta = 0, \pi) = \epsilon_\parallel(\theta = 0, \pi) = 1$, as a consequence of the boost invariance.

Let us further assume that the scalar functions χ_i have imaginary parts. Then, the dielectric constants also have imaginary parts: $\epsilon = \epsilon_{\rm real} + i\,\epsilon_{\rm imag}$. We will see later in Sec. IV that imaginary parts indeed appear under some kinematical conditions. Since the dielectric constants and refractive indices are related with each other via $n^2 = \epsilon$, we can similarly define real and imaginary parts of the refractive indices:[8]

$$n = n_{\rm real} + i\, n_{\rm imag} \quad , \tag{25}$$

where one can easily find ($|\epsilon| = \sqrt{\epsilon_{\rm real}^2 + \epsilon_{\rm imag}^2}$)

$$n_{\rm real} \;=\; \frac{1}{\sqrt{2}}\sqrt{|\epsilon| + \epsilon_{\rm real}}\,, \tag{26}$$

$$n_{\rm imag} \;=\; \frac{1}{\sqrt{2}}\sqrt{|\epsilon| - \epsilon_{\rm real}}\,. \tag{27}$$

While a purely real dielectric constant yields a real refractive index[9] $n_{\rm real} = \sqrt{\epsilon_{\rm real}}$, a purely imaginary dielectric constant leads to an equal magnitude of real and imaginary parts, $n_{\rm real} = n_{\rm imag} = \sqrt{|\epsilon|/2}$ with $|\epsilon| = |\epsilon_{\rm imag}|$. In Appendix D, we have explained that real and imaginary parts of the two refractive indices $n_\parallel$ and $n_\perp$ in general provide distinct phase velocities and extinction coefficients of physical modes $\lambda = 1, 2$ in Eq. (20), respectively.

It should be noticed and taken care of carefully that the right-hand sides of Eqs. (23) and (24) depend on the dielectric constants $\epsilon_\perp$ and $\epsilon_\parallel$, respectively, through the photon

[8] Since there are two polarization modes, one can define two different refractive indices $n_\parallel$ and $n_\perp$, both of which can be complex quantities.

[9] Inserting Eqs. (23) and (24) into this expression and then expanding them with respect to $\chi_0 \sim 0$, $\chi_1 \ll 1$, and $\chi_2 \ll 1$, we obtain approximate forms shown in literatures, $n_\perp = 1 - (\chi_2/2)\sin^2\theta$ and $n_\parallel = 1 + (\chi_1/2)\sin^2\theta$. However, one should bear in mind that χ_0, χ_1 and χ_2 can be even divergent and complex depending on kinematical variables, as we will see in Sec. IV.

momenta $r_\parallel^2$ and $r_\perp^2$. According to the definition of the dielectric constant (22), those momenta are written as $r_\parallel^2 = \tilde{\omega}^2(1 - \epsilon\cos^2\theta)$ and $r_\perp^2 = -\epsilon\,\tilde{\omega}^2\sin^2\theta$, where we introduced a normalized photon energy $\tilde{\omega}^2 = \omega^2/(4m^2)$. Thus, if one wants to obtain the dielectric constant ϵ as a function of the photon energy $\tilde{\omega}$, Eqs. (23) and (24) have to be solved with respect to ϵ. Physically, this structure reflects effects of a back-reaction appearing as screening of an incident photon field by an induced vacuum polarization, which should be taken into account self-consistently when the magnitude of the polarization becomes large. As mentioned above, the dielectric constants are in general complex, and thus damping of the incident photon field, due to the decay into a fermion-antifermion pair, should also be treated self-consistently. Therefore, we need to simultaneously solve two sets of coupled equations (obtained from Eqs. (23) and (24)) for the real and imaginary parts of $\epsilon_\perp$ and $\epsilon_\parallel$ in a self-consistent way. There are indeed kinematical regions where these procedures play an important role to correctly obtain the dielectric constant. We will explicitly demonstrate it in the next paper [22].

IV. ANALYTIC EVALUATION OF THE VACUUM POLARIZATION TENSOR

In the previous sections, we have discussed in a formal way that a nonzero vacuum polarization tensor in a magnetic field necessarily gives rise to the vacuum birefringence. In order to know how large the effect is and how it depends on kinematical conditions, we have to explicitly evaluate the scalar functions χ_i $(i = 0, 1, 2)$ of which formal expressions were already given in Eqs. (9) – (11). Notice that this representation contains somewhat complicated integration with respect to β and τ, corresponding to the difference and the average of two proper-time variables. In fact, this complexity has prevented previous studies from complete analytical understanding of the vacuum birefringence [16, 17, 19], and even from performing numerical computation except in a limited kinematical region [18]. We will, in this section, perform the integration *analytically* by rewriting the integrand into a double infinite series of familiar functions, and show that the infinite series indeed has a physical meaning. We will see that the scalar functions χ_i and thus the refractive indices are sensitively affected by microscopic structure of the fermion spectrum in a magnetic field, i.e., the Landau levels formed by the fermions. Therefore, as in optics for materials, macroscopic electromagnetism of the vacuum should be elucidated by the microscopic dynamics of the

Dirac sea which is excited by an incident photon field.

A. Computing the scalar functions χ_i

Before we present the procedures how to analytically perform the integrals, let us briefly point out technical difficulties in the integral representation, Eqs. (9) – (11). Note that each integrand in χ_i contains an exponential function whose argument is given by trigonometric functions. This factor causes strong oscillation of the integrand composed of arbitrarily higher harmonics, because k-th power of the trigonometric function that appears in a Taylor expansion of the exponential factor is composed of higher harmonics up to k times the fundamental frequency. For example, the factor $\mathrm{e}^{i\eta\cot\tau}$ contains a term proportional to $\cos^3\tau$ at $k=3$ in the Taylor expansion, which is composed of up to the 3rd higher harmonics as $\cos^3\tau = \{3\cos\tau + \cos(3\tau)\}/4$. In general, this strong oscillation even cannot be periodic due to mixing of two fundamental periods, 2π and $2\pi/\beta$. These complicacies, directly or indirectly, cause difficulties in analytic and numerical evaluations of the integral. In fact, as we will see later, results of the integration have singular behaviors at some kinematical conditions, which may invalidate numerical approaches.

The first thing to overcome this situation is to rewrite the integrand so that the exponential function does not contain trigonometric functions of the fundamental period, $2\pi/\beta$ (Step I). We will still have an exponential function with a trigonometric function in the argument which is however composed of a unique fundamental period, 2π. We can rewrite it by a series expansion so that the exponential function does not contain any trigonometric function (Step II). The resultant integrand will allow us to easily perform analytic integration (Step III). Below, we explain these procedures step by step.

1. Step I: Partial wave decomposition

Consider the functions in the integrand in Eq. (9) that depend on trigonometric functions with a fundamental period $2\pi/\beta$. Namely, $\mathrm{e}^{-iu\cos(\beta\tau)}$, $\cos(\beta\tau)\mathrm{e}^{-iu\cos(\beta\tau)}$, and $\cos(\beta\tau)\mathrm{e}^{-iu\cos(\beta\tau)}$. We can equivalently rewrite these functions by using the partial wave decomposition [26].

By adopting the formulae given in Appendix E, we obtain the following[10]:

$$\chi_i = \frac{\alpha}{4\pi}\int_{-1}^{1}d\beta\int_0^\infty d\tau\ \sum_{n=0}^{\infty}(2-\delta_{n0})\frac{\gamma_i^{(n)}(\tau,\beta)}{\sin\tau}\ \mathrm{e}^{i\eta\cot\tau}\,\mathrm{e}^{-i(\phi_\parallel-n\beta)\tau}\,, \tag{28}$$

with $\gamma_i^{(n)}(\tau,\beta)$ defined by

$$\begin{aligned}
\gamma_0^{(n)}(\tau,\beta) &\equiv \frac{1}{2}\left\{\, I_{n+1}(-iu)+I_{n-1}(-iu)\,\right\} - n\beta\ \eta^{-1}I_n(-iu)\cos\tau\,,\\
\gamma_1^{(n)}(\tau,\beta) &\equiv (1-\beta^2)I_n(-iu)\cos\tau-\gamma_0^{(n)}(\tau,\beta)\,,\\
\gamma_2^{(n)}(\tau,\beta) &\equiv \sin^{-2}\tau\left\{\, I_{n+1}(-iu)+I_{n-1}(-iu)-2I_n(-iu)\cos\tau\,\right\}-\gamma_0^{(n)}(\tau,\beta)\,,
\end{aligned} \tag{29}$$

where $I_n(-iu)$ is the modified Bessel function of the first kind. Except for the last trivial exponential factor $\mathrm{e}^{-i(\phi_\parallel-n\beta)\tau}$ in Eq. (28), the integrand now oscillates with the fundamental period 2π. Note that $I_n(-iu)$ also oscillates with the fundamental period 2π because its argument is proportional to cosecant as, $-iu=-i\eta\csc\tau$.

2. Step II: Infinite series expansion

We are able to further simplify the integrand by using the following technique. We first introduce a variable z defined by

$$z\equiv\exp(-2i\tau)\,.$$

Then, a product of the exponentiated cotangent and the modified Bessel function in Eqs. (28) and (29) are rewritten as $\mathrm{e}^{i\eta\cot\tau}\ I_n(-iu)=\mathrm{e}^{-\eta}\mathrm{e}^{-z\frac{2\eta}{1-z}}\ I_n(\frac{2(\eta^2z)^{\frac{1}{2}}}{1-z})$. We use the following formula which is deduced from the relation between confluent geometrical functions [27]:

$$\exp\left(-z\frac{x+y}{1-z}\right)I_n\left(\frac{2(xyz)^{\frac{1}{2}}}{1-z}\right)=(1-z)\,(xyz)^{\frac{n}{2}}\sum_{\ell=0}^{\infty}\frac{\ell!}{\Gamma(\ell+n+1)}\ L_\ell^n(x)L_\ell^n(y)\ z^\ell\,, \tag{30}$$

where $L_\ell^n(x)$ and $\Gamma(x)$ are the associated Laguerre polynomial and the Gamma function, respectively. Notice that this relation disentangles the function with a nontrivial z-dependence (left-hand side) into a sum of polynomials of z (right-hand side), which is quite useful for the present purpose. Namely, the resulting integrand can be now written only in terms of simple exponentials of τ. Taking parameters in the above formula as $x=y=\eta$ and

[10] We just use the partial wave decomposition as a mathematical tool. Later, the index n is interpreted as a physical quantity, but not an angular momentum.

using $(1-z)^{-2} = \sum_{i=0}^{\infty}\sum_{j=0}^{\infty} z^{i+j} = \sum_{k=0}^{\infty}(k+1)\ z^k$, we find that the double integrals are simplified to either of the following representations:

$$F_\ell^n(r_\parallel^2, B_{\rm r}) \equiv \frac{i}{B_{\rm r}}\int_{-1}^{1} d\beta \int_0^\infty d\tau\ {\rm e}^{-i\left(\phi_\parallel + 2\ell - n\beta + n\right)\tau}\,, \tag{31}$$

$$G_\ell^n(r_\parallel^2, B_{\rm r}) \equiv \frac{i}{B_{\rm r}}\int_{-1}^{1} d\beta \int_0^\infty d\tau\ \beta\,{\rm e}^{-i\left(\phi_\parallel + 2\ell - n\beta + n\right)\tau}\,, \tag{32}$$

$$H_\ell^n(r_\parallel^2, B_{\rm r}) \equiv \frac{i}{B_{\rm r}}\int_{-1}^{1} d\beta \int_0^\infty d\tau\ \beta^2\,{\rm e}^{-i\left(\phi_\parallel + 2\ell - n\beta + n\right)\tau}\,. \tag{33}$$

Appart from these integrals, we have nontrivial coefficients which contain the associated Laguerre polynomials as we will explicitly show in the final expression below. Here we just emphasize that, thanks to the formula (30), the longitudinal ($r_\parallel^2$) dependence of $\chi_i(r_\parallel^2, r_\perp^2)$ appears only in the functions F, G and H, while the transverse ($r_\perp^2$) dependence are factorized and appears in the other parts.

3. Step III: Performing double integrals

The integrals in Eqs. (31) – (33) are simple enough and we can carry out integration analytically. However, it should be noticed that these integrals contain singular behaviors, which appear when the exponential factor becomes unity due to a vanishing argument. Depending on the photon momentum $r_\parallel^2$, there arises such a divergent contribution within the integral region, $\beta \in [-1, 1]$. A simple way to obtain the integrals with respect to any $r_\parallel^2$ is provided by the technique of analytic continuation. First, assuming that the rescaled photon momentum $r_\parallel^2$ satisfies $\phi_\parallel(r_\parallel^2, B_{\rm r}) + (2\ell - n\beta + n) > 0$, we perform convergent integration by rotating the contour in the complex τ-plane downward. Then, analytic continuation allows us to inspect the analytic property afterward. At this moment, the τ-integral is carried out as follows:

$$F_\ell^n(r_\parallel^2, B_{\rm r}) = \int_{-1}^{1} \frac{d\beta}{r_\parallel^2\beta^2 - nB_{\rm r}\beta + (1 - r_\parallel^2) + (2\ell + n)B_{\rm r}} \equiv I_{\ell\Delta}^n(r_\parallel^2)\quad . \tag{34}$$

The integral with respect to β simply provides a difference $I_{\ell\Delta}^n(r_\parallel^2) = I_{\ell+}^n(r_\parallel^2) - I_{\ell-}^n(r_\parallel^2)$ between the following functions:

$$I_{\ell\pm}^n(r_\parallel^2) \equiv \frac{2}{\sqrt{4ac - b^2}}\arctan\left(\frac{b \pm 2a}{\sqrt{4ac - b^2}}\right)\quad . \tag{35}$$

We have introduced parameters $a = r_\parallel^2$, $b = -nB_{\rm r}$ and $c = (1 - r_\parallel^2) + (2\ell + n)B_{\rm r}$, and the integral with respect to β has been carried out in a regime, $4ac - b^2 > 0$. Note that the

condition for $r_\parallel^2$ assumed above involves this regime. Similarly, the remaining other two integrals are performed as [11]

$$G_\ell^n(r_\parallel^2, B_{\rm r}) = \frac{1}{2r_\parallel^2}\left[\ \Xi_\ell^n(B_{\rm r}) + nB_{\rm r}\ I_{\ell\Delta}^n(r_\parallel^2)\ \right], \tag{36}$$

$$H_\ell^n(r_\parallel^2, B_{\rm r}) = \frac{1}{r_\parallel^2}\left[\ 2 + \frac{nB_{\rm r}}{2r_\parallel^2}\ \Xi_\ell^n(B_{\rm r}) + \frac{1}{4r_\parallel^2}\left\{\ (b^2-4ac) + (nB_{\rm r})^2\ \right\} I_{\ell\Delta}^n(r_\parallel^2)\ \right], \tag{37}$$

where we have introduced a real constant Ξ (i.e., independent of kinematical variables):

$$\Xi_\ell^n(B_{\rm r}) \equiv \ln\left|\frac{1+2\ell B_{\rm r}}{1+2(\ell+n)B_{\rm r}}\right| = \ln\left|\frac{m^2+2\ell eB}{m^2+2(\ell+n)eB}\right|.$$

We have performed the integrals under the condition $4ac - b^2 > 0$. However, the obtained results can be analytically continued to the regime $4ac - b^2 < 0$, where the function $I_{\ell\Delta}^n(r_\parallel^2)$ will become complex as we will see later.

4. Final results

Now that we have performed all the integrals, we find the analytic expression of χ_i $(i = 0, 1, 2)$. In order to present the results in a compact form, let us define the coefficients $C_\ell^n(\eta)$ expressed by the associated Lagguerre polynomials[12]:

$$C_\ell^n(\eta) \equiv {\rm e}^{-\eta}\frac{\ell!}{(\ell+n)!}\,\eta^n\left[L_\ell^n(\eta)\right]^2. \tag{38}$$

Then, the coefficients χ_i of the vacuum polarization tensor (7) are finally represented as the infinite sum of known functions as

$$\chi_i = \frac{\alpha B_{\rm r}}{4\pi}\sum_{n=0}^{\infty}(2-\delta_{n0})\left[\ \sum_{\ell=0}^{\infty}\Omega_{\ell i}^{n(0)} + \sum_{\ell=1}^{\infty}\Omega_{\ell i}^{n(1)} + \sum_{\ell=2}^{\infty}\Omega_{\ell i}^{n(2)}\ \right], \tag{39}$$

where we have introduced three functions $\Omega_{\ell i}^{n(0)}$, $\Omega_{\ell i}^{n(1)}$, and $\Omega_{\ell i}^{n(2)}$, as we define below.

For $i = 0$, they are defined as

$$\Omega_{\ell 0}^{n(0)} = (1-\delta_{n0})\ C_\ell^{n-1}(\eta)\ F_\ell^n(\xi, B_{\rm r}) - n\eta^{-1}\ C_\ell^n(\eta)\ G_\ell^n(\xi, B_{\rm r}),$$

$$\Omega_{\ell 0}^{n(1)} = (1+\delta_{n0})\ C_{\ell-1}^{n+1}(\eta)\ F_\ell^n(\xi, B_{\rm r}) - \ n\eta^{-1}\ C_{\ell-1}^n(\eta)\ G_\ell^n(\xi, B_{\rm r}),$$

[11] Although the expressions of $G_\ell^n(r_\parallel^2, B_{\rm r})$ and $H_\ell^n(r_\parallel^2, B_{\rm r})$ apparently look singular at $r_\parallel^2 = 0$, one can check that both of them are regular there.

[12] We employ a convention for the associated Laguerre polynomial defined by series: $L_\ell^n(\eta) = \frac{{\rm e}^\eta \eta^{-n}}{\ell!}\frac{d^\ell}{d\eta^\ell}\left({\rm e}^{-\eta}\eta^{\ell+n}\right) = \sum_{r=0}^{\ell}\ {}_{\ell+n}{\rm C}_{\ell-r}\ \frac{(-\eta)^r}{r!}$.

$$\Omega^{n(2)}_{\ell\,0} = 0\,. \tag{40}$$

Note that the functions F and G (and also H) depend on $r_\parallel^2$ only through the combination, $\xi \equiv 2r_\parallel^2/B_{\rm r}$. Thus, we have written them as $F(\xi, B_{\rm r})$ and $G(\xi, B_{\rm r})$. Similarly, for $i = 1$, we have

$$\begin{aligned}
\Omega^{n(0)}_{\ell\,1} &= C^n_\ell(\eta)\left\{F^n_\ell(\xi, B_{\rm r}) - H^n_\ell(\xi, B_{\rm r})\right\} - \Omega^{n(0)}_{\ell\,0}\,,\\
\Omega^{n(1)}_{\ell\,1} &= C^n_{\ell-1}(\eta)\left\{F^n_\ell(\xi, B_{\rm r}) - H^n_\ell(\xi, B_{\rm r})\right\} - \Omega^{n(1)}_{\ell\,0}\,,\\
\Omega^{n(2)}_{\ell\,1} &= 0\,,
\end{aligned} \tag{41}$$

and finally for $i = 2$,

$$\begin{aligned}
\Omega^{n(0)}_{\ell\,2} &= -\Omega^{n(0)}_{\ell\,0}\,,\\
\Omega^{n(1)}_{\ell\,2} &= \ D^{n(1)}_\ell(\eta)\ F^n_\ell(\xi, B_{\rm r}) - \Omega^{n(1)}_{\ell\,0}\,,\\
\Omega^{n(2)}_{\ell\,2} &= \ D^{n(2)}_\ell(\eta)\ F^n_\ell(\xi, B_{\rm r})\,.
\end{aligned} \tag{42}$$

In the last expression, we introduced coefficient functions $D^{(1)}$ and $D^{(2)}$ defined by

$$D^{n(1)}_\ell(\eta) = -8\sum_{\lambda=0}^{\ell-1}\ (\ell-\lambda)\left\{(1-\delta_{n0})\ C^{n-1}_\lambda(\eta) - C^n_\lambda(\eta)\right\}\,, \tag{43}$$

$$D^{n(2)}_\ell(\eta) = -8\sum_{\lambda=0}^{\ell-2}\ (\ell-\lambda-1)\left\{(1+\delta_{n0})\ C^{n+1}_\lambda(\eta) - C^n_\lambda(\eta)\right\}\,. \tag{44}$$

These are the final analytic results represented as an infinite series of known functions. For fixed n and ℓ, each term in the expansion is finite (except for some special kinematical points as we will discuss soon). The ultraviolet divergence of the function χ_0 appears only after one takes the infinite summation (see Appendix B).

Figure 3 shows ℓ-dependence of the coefficient $C^n_\ell(\eta)$ in Eq. (38) at fixed η and n. The associated Laguerre polynomial provides an oscillation, and, in case of finite n, a ratio of the factorials strongly suppresses $C^n_\ell(\eta)$ for small ℓ. In Appendix F, we discuss the behavior of $C^n_\ell(\eta)$ in the limit of large $\ell \gg 1$. By using the limiting form (F5) of $C^n_\ell(\eta)$ at large values of ℓ with fixed η and n, one can put the upper bound for $C^n_\ell(\eta)$:

$$0 \le C^n_\ell(\eta) \le \frac{1}{\pi\sqrt{\eta\ell}}\,{\rm e}^{-\frac{n+1}{2\ell}} \quad (\ell \gg 1)\,, \tag{45}$$

Black dashed line shows the upper bound of $C^n_\ell(\eta)$ for $n = 0$, and the other two cases are also bounded at large ℓ outside the plot range. While the upper bound in Eq. (45) indicates

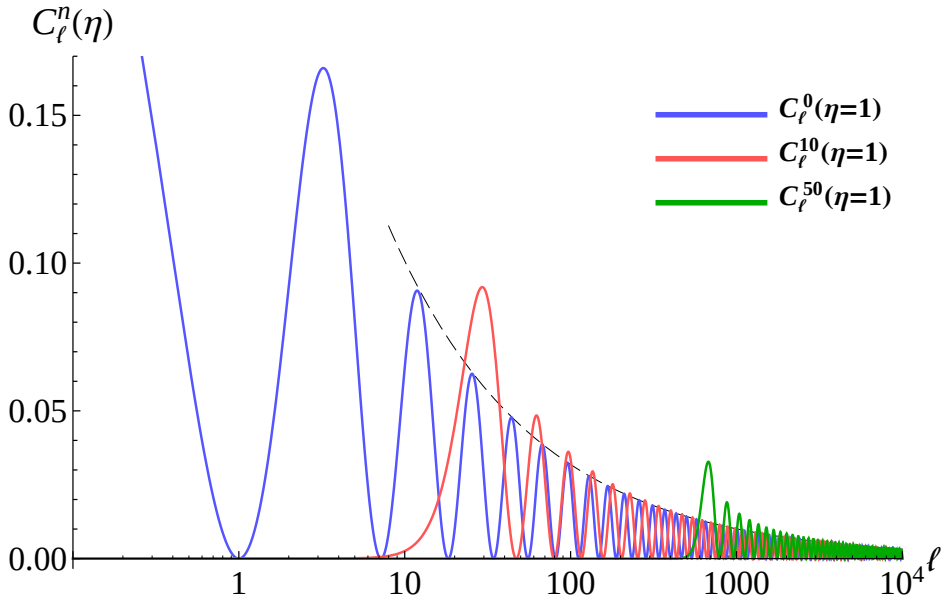

FIG. 3. Coefficient $C_\ell^n(\eta)$ at fixed n and η: $C_\ell^n(\eta)$ at discrete ℓ takes a value on curves plotted against continuous ℓ. A dashed line shows the upper bound for the coefficient at $n = 0$ that is valid at large $\ell \gg 1$. Owing to Eq. (F5), other two curves are also bounded at large ℓ outside the plot range. Note that the coefficient has a finite value at $\ell = 0$ given by $C_0^n(\eta) = \mathrm{e}^{-\eta}\eta^n/n!$.

that $C_\ell^n(\eta)$ for large ℓ converges to zero by an inverse-square-root, this suppression is not sufficiently strong to guarantee a convergence of the infinite sum (39). Indeed, we find a logarithmic divergence of the function χ_0 by carrying out the infinite sum. However, the logarithmic divergence has been foreseen *a priori* to appear in terms of the ultraviolet divergence mentioned below Eq. (11), which should be removed by an appropriate prescription (see Appendix B).

B. Physical meaning of the results: Landau levels

The use of infinite series expansion was motivated rather by technical reasons for making the double integrals simpler. However, as we will see below, the indices ℓ and n in the expansions have well-defined physical meaning: they are related to the Landau levels of the fermion-antifermion pair which appears in the one-loop diagram shown in Fig. 2.

First of all, it should be noticed that an important kinematical property of the scalar function χ_i, with respect to $r_\parallel^2$, is essentially determined by the function $I_{\ell\Delta}^n(r_\parallel^2)$ which is

the only one possible source of an imaginary part. Therefore, we investigate the structure of $I^n_{\ell\Delta}(r_\parallel^2)$ in order to understand kinematics in the presence of an external magnetic field, and to identify the physical meaning of the indices ℓ and n.

A kinematical property of $I^n_{\ell\Delta}(r_\parallel^2)$ is specified by a discriminant appearing in Eq (35):

$$\begin{aligned}\mathcal{D} &\equiv b^2 - 4ac \\ &= (-nB_{\rm r})^2 - 4r_\parallel^2\left[(1-r_\parallel^2) + (2\ell+n)B_{\rm r}\right] \ . \end{aligned} \tag{46}$$

Depending on the sign of $\mathcal{D}$, arguments of the arctangent in $I^n_{\ell\Delta}(r_\parallel^2)$ are either real or pure imaginary. Solving an equality, $\mathcal{D}=0$, we find boundaries of the momentum region specified by a pairwise solution,

$$r_\parallel^2 = \frac{1}{4}\left\{\sqrt{1+2\ell B_{\rm r}} \pm \sqrt{1+2(\ell+n)B_{\rm r}}\right\}^2 \equiv s_\pm^{\ell n} \ . \tag{47}$$

If the photon momentum resides in the regime $s_-^{\ell n} < r_\parallel^2 < s_+^{\ell n}$ where $\mathcal{D}>0$, the function $I^n_{\ell\Delta}(r_\parallel^2)$ is obviously a real-valued function. On the other hand, in the other regimes, $r_\parallel^2 < s_-^{\ell n}$ and $s_+^{\ell n} < r_\parallel^2$ where $\mathcal{D}<0$, it possibly becomes a complex function. However, we show in Appendix G that $I^n_{\ell\Delta}(r_\parallel^2)$ has an imaginary part only if the photon momentum resides in the higher regime, $s_+^{\ell n} < r_\parallel^2$. In other words, it does not have an imaginary part in the complementary regime, $r_\parallel^2 < s_+^{\ell n}$ which includes $r_\parallel^2 < s_-^{\ell n}$. After careful investigation shown in Appendix G, we obtain a piecewise representation as,

$$I^n_{\ell\Delta}(r_\parallel^2) = \begin{cases} \frac{1}{\sqrt{(r_\parallel^2 - s_-^{\ell n})(r_\parallel^2 - s_+^{\ell n})}} \cdot \frac{1}{2}\ln\left|\frac{a-c-\sqrt{b^2-4ac}}{a-c+\sqrt{b^2-4ac}}\right| & (r_\parallel^2 < s_-^{\ell n}) \\ \frac{1}{\sqrt{\left|(r_\parallel^2 - s_-^{\ell n})(r_\parallel^2 - s_+^{\ell n})\right|}}\left[\arctan\left(\frac{b+2a}{\sqrt{4ac-b^2}}\right) - \arctan\left(\frac{b-2a}{\sqrt{4ac-b^2}}\right)\right] & (s_-^{\ell n} < r_\parallel^2 < s_+^{\ell n}) \\ \frac{1}{\sqrt{(r_\parallel^2 - s_-^{\ell n})(r_\parallel^2 - s_+^{\ell n})}} \cdot \frac{1}{2}\left[\ \ln\left|\frac{a-c-\sqrt{b^2-4ac}}{a-c+\sqrt{b^2-4ac}}\right| + 2\pi i\ \right] & (s_+^{\ell n} < r_\parallel^2)\,. \end{cases} \tag{48}$$

An imaginary part in $I^n_{\ell\Delta}(r_\parallel^2)$ results in the imaginary part of the scalar functions χ_i, and of the vacuum polarization tensor $\Pi^{\mu\nu}_{\rm ex}(q)$. Consequently, the dielectric constants and thus refractive indices have imaginary parts as alluded in Eqs. (23) – (27). They represent damping of photon propagation in the presence of an external magnetic field. As foreseen owing to the optical theorem, this damping is caused by decay into a fermion-antifermion pair. Thus, we interpret $r_\parallel^2 = s_+^{\ell n}$ as the threshold momentum of photon decay, and notice that there are infinite number of threshold momenta as the indices ℓ and n run from zero to infinity.

In terms of dimensionful quantities, the threshold condition $r_\parallel^2 = s_+^{\ell n}$ for the photon decay is expressed as

$$q_\parallel^2 = \left\{ \sqrt{m^2 + 2\ell eB} + \sqrt{m^2 + 2(\ell + n)eB} \right\}^2 . \tag{49}$$

Recall that the energy of a charged particle in a magnetic field is $\varepsilon_n(p_z) = \sqrt{m^2 + p_z + 2neB}$. This immediately implies that the right-hand side of Eq. (49) exactly agrees with the invariant mass of a fermion-antifermion pair carrying quantized transverse momenta in the magnetic field and vanishing longitudinal momenta along the external field. The integers ℓ and $\ell + n$ specify the Landau levels.

Reflecting the boost invariance of the system along the external constant magnetic field, the left-hand side of Eq. (49) has a boost invariant form $q_\parallel^2$. It indicates that the decay condition should be invariant in a class of Lorentz frames which are connected by the boost along the external field, because the propagating photon receives an influence from the magnetic field of the same configuration. Owing to the boost invariance, it is possible, without varying the configuration of the external field, to take the Lorentz frame in which the longitudinal momentum of the photon vanishes,[13] $q_{(0)z} = 0$. In this Lorentz frame, we have $q_\parallel^2 = \omega_{(0)}^2 - q_{(0)z}^2 = \omega_{(0)}^2$, and the condition (49) represents nothing but the smallest photon energy to produce a fermion-antifermion pair in the Landau levels ℓ and $\ell + n$ with vanishing longitudinal momenta.

For each ℓ and n, the function $I_\ell^n(r_\parallel^2)$ has a single threshold momentum beyond which a photon can decay into a fermion-antifermion pair with the Landau levels specified by ℓ and $\ell + n$. Since the coefficients χ_i and thus the vacuum polarization tensor are given as the infinite sum of $I_\ell^n(r_\parallel^2)$ over the indices ℓ and n, there are infinite number of threshold momenta in the photon momentum $r_\parallel^2$. Beyond the each threshold momentum, the vacuum polarization tensor has an imaginary part, indicating a branch cut continuously running on the real axis in the complex $q_\parallel^2$-plane. The half line of the cut and its starting point at the threshold correspond to the continuous and vanishing longitudinal momenta of a real pair excitation from the vacuum, respectively.

In order to confirm our interpretation of the Landau levels, let us look at the contribution from the lowest Landau levels, $\ell = n = 0$. Taking $\ell = n = 0$ in Eq. (39), we find that the

[13] If one wants to perform an equivalent analysis in a Lorentz frame disconnected to this class, one has to take into account an electric field orthogonal to the magnetic field.

coefficients χ_i of the vacuum polarization tensor survive only for $i = 1$. Namely, they read $\chi_0 = \chi_2 = 0$, and

$$\chi_1(r_\parallel^2, r_\perp^2; B_{\rm r}) = \frac{\alpha B_{\rm r}}{4\pi}\, {\rm e}^{-\eta} \times \frac{1}{r_\parallel^2}\left\{ I_{0\Delta}^0(r_\parallel^2) - 2 \right\} , \tag{50}$$

where we have used $L_0^0(\eta) = 1$. Depending on the values of $r_\parallel^2$ (the boundaries are $s_-^{00} = 0$ and $s_+^{00} = 1$ (or, $q_\parallel^2 = 4m^2$), see Eq. (47)), the piecewise expression of $I_{0\Delta}^0(r_\parallel^2)$ follows from Eq. (48) as

$$I_{0\Delta}^0(r_\parallel^2) = \begin{cases} \frac{1}{\sqrt{r_\parallel^2(r_\parallel^2-1)}} \ln \left| \frac{r_\parallel^2 - \sqrt{r_\parallel^2(r_\parallel^2-1)}}{r_\parallel^2 + \sqrt{r_\parallel^2(r_\parallel^2-1)}} \right| & (r_\parallel^2 < 0) \\ \frac{2}{\sqrt{r_\parallel^2(1-r_\parallel^2)}} \arctan \left\{ \frac{r_\parallel^2}{\sqrt{r_\parallel^2(1-r_\parallel^2)}} \right\} & (0 < r_\parallel^2 < 1) \\ \frac{1}{\sqrt{r_\parallel^2(r_\parallel^2-1)}} \left[\ln \left| \frac{r_\parallel^2 - \sqrt{r_\parallel^2(r_\parallel^2-1)}}{r_\parallel^2 + \sqrt{r_\parallel^2(r_\parallel^2-1)}} \right| + \pi i \right] & (1 < r_\parallel^2) \end{cases} . \tag{51}$$

Notice that this result does not depend on $B_{\rm r}$, reflecting the fact that the threshold condition $q_\parallel^2 = 4m^2$ is independent of $B_{\rm r}$.

In principle, one could compute the vacuum polarization tensor by an alternative method. By using fermion propagators which are decomposed into the Landau levels [28, 29], the one-loop diagram can be calculated order-by-order with respect to the Landau levels. The outcome would however look rather complicated compared with our calculation in the proper-time method. Nevertheless, as far as the lowest Landau level is concerned, a simple calculation leads to an analytic expression of the vacuum polarization tensor at this level. This calculation was recently carried out in Ref. [30], and the result is exactly the same as above. Therefore, our analytic results correctly reproduce the lowest Landau level contribution, suggesting the legitimacy of our interpretation of the Landau levels.

Note that the vacuum birefringence is specified by the external photon momentum and the magnitude of the external magnetic field. Then, we notice that the lowest Landau level contribution is not necessarily enough for the calculation of the dielectric constants and refractive indices of energetic photons. Figure 4 shows variation of the threshold structure with increasing magnetic field $B_{\rm r}$. The vertical line corresponds to the longitudinal photon momentum squared $r_\parallel^2 = q_\parallel^2/(4m^2)$, and curves show locations of the thresholds $r_\parallel^2 = s_+^{\ell n}$. We have shown only up to the 14th threshold. The high momentum region above the 14th threshold line (i.e., the shaded region) is filled with narrowly spaced many curves. This figure visualizes that there is certainly a region (i.e., low momentum and strong field) where

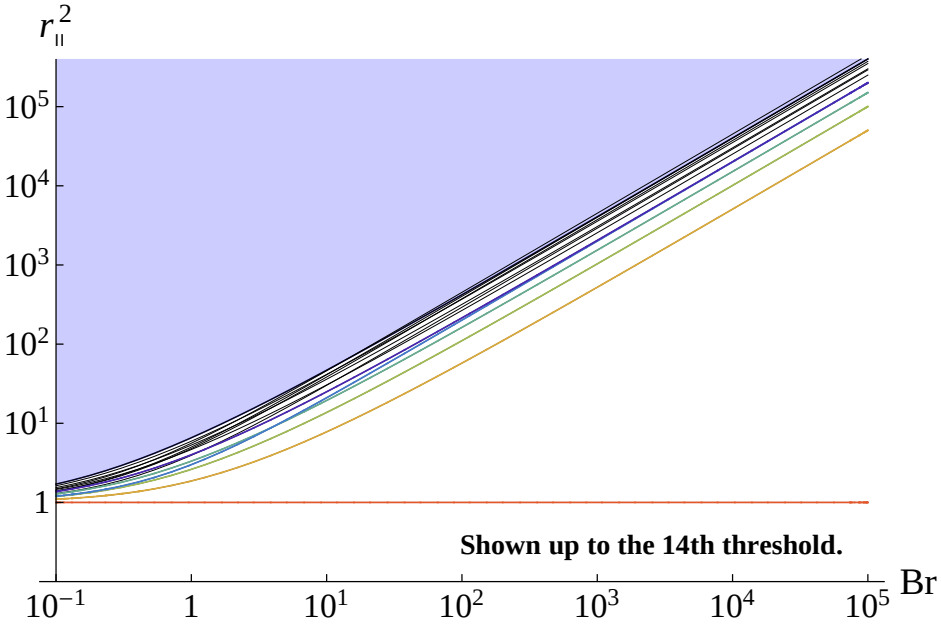

FIG. 4. Threshold structure of photon momentum as a function of $B_{\rm r}$. Curves are positions of thresholds $r_\parallel^2 = s_+^{\ell n}$. We have shown threshold lines from the lowest (horizontal line at $r_\parallel^2 = 1$) up to the 14th. With increasing $B_{\rm r}$, the lowest threshold is isolated from higher levels more distantly, and thus the lowest Landau level approximation is justified in a wider kinematical region below the second threshold.

the lowest Landau level approximation is appropriate. However, if a photon momentum $r_\parallel^2$ approaches higher levels, the levels close to the photon momentum would provide dominant contributions and thus higher-level contributions have to be incorporated in calculations even in strong magnetic field limits. With the results of a series representation in Eq. (39), important contributions from individual Landau levels can be systematically taken into account in calculating the vacuum polarization tensor.

C. Behavior of the coefficients χ_i at the thresholds

Let us carefully see the behavior of the function $I^n_{\ell\Delta}(r_\parallel^2)$ at the boundaries $r_\parallel^2 = s_\pm^{\ell n}$, which should be essentially the same as those of the coefficients χ_i. First of all, given the explicit form of $I^n_{\ell\Delta}(r_\parallel^2)$ in Eq. (48), one might expect that singularities could appear at both of the boundaries due to the inverse-square-root. But in fact, one finds that $I^n_{\ell\Delta}(r_\parallel^2)$ is smooth

at the lower boundary $r_\parallel^2 = s_-^{\ell n}$ while it has a discontinuity with divergence at the higher boundary $r_\parallel^2 = s_+^{\ell n}$ (see Appendix H for more details).

As $r_\parallel^2$ approaches the lower boundary $r_\parallel^2 = s_-^{\ell n}$ from below and above, one finds that the values of $I^n_{\ell\Delta}(r_\parallel^2)$ are finite and coincide with each other:

$$\lim_{r_\parallel^2 \to s_-^{\ell n} - 0} I^n_{\ell\Delta}(r_\parallel^2) = \lim_{r_\parallel^2 \to s_-^{\ell n} + 0} I^n_{\ell\Delta}(r_\parallel^2) = \left. \frac{2}{c-a} \right|_{r_\parallel^2 = s_-^{\ell n}} = 2\rho(\ell, n; B_{\rm r})\,, \tag{52}$$

where a limiting value is given by $\rho(\ell, n; B_{\rm r}) = \{(1+2\ell B_{\rm r})(1+2(\ell+n)B_{\rm r})\}^{-1/2}$. Note that this is a real number as we commented before. On the other hand, if $r_\parallel^2$ goes beyond the higher boundary $r_\parallel^2 = s_+^{\ell n}$ (threshold for the photon decay), the function $I^n_{\ell\Delta}(r_\parallel^2)$ has an imaginary part. Then we find that both the real and imaginary parts of $I^n_{\ell\Delta}(r_\parallel^2)$ show singular behavior at the higher boundary $r_\parallel^2 = s_+^{\ell n}$. The real part goes

$$\lim_{r_\parallel^2 \to s_+^{\ell n} - 0} I^n_{\ell\Delta}(r_\parallel^2) \;\; = \lim_{r_\parallel^2 \to s_+^{\ell n} - 0} \frac{\lambda(r_\parallel^2)}{\sqrt{s_+^{\ell n} - r_\parallel^2}} = +\infty\,, \tag{53}$$

$$\lim_{r_\parallel^2 \to s_+^{\ell n} + 0} {\rm Re}\left[I^n_{\ell\Delta}(r_\parallel^2)\right] = \left. \frac{2}{c-a} \right|_{r_\parallel^2 = s_+^{\ell n}} = -2\rho(\ell, n; B_{\rm r})\,, \tag{54}$$

where the coefficient $\lambda(r_\parallel^2) \equiv \pi(r_\parallel^2 - s_-^{\ell n})^{-1/2}$ takes a finite positive value at the threshold, $\lambda(s_+^{\ell n}) = \pi\rho^{\frac{1}{2}}(\ell, n; B_{\rm r})$. On the other hand, the imaginary part diverges as $r_\parallel^2$ approaches $r_\parallel^2 = s_+^{\ell n}$ from above, while it is just zero from below:

$$\lim_{r_\parallel^2 \to s_+^{\ell n} - 0} {\rm Im}\left[I^n_{\ell\Delta}(r_\parallel^2)\right] = 0\,, \tag{55}$$

$$\lim_{r_\parallel^2 \to s_+^{\ell n} + 0} {\rm Im}\left[I^n_{\ell\Delta}(r_\parallel^2)\right] = \lim_{r_\parallel^2 \to s_+^{\ell n} + 0} \frac{\lambda(r_\parallel^2)}{\sqrt{r_\parallel^2 - s_+^{\ell n}}} = +\infty\,. \tag{56}$$

Such singular behavior appears only at the higher boundary $r_\parallel^2 = s_+^{\ell n}$ for each number of ℓ and n. The finite value $\rho(\ell, n; B_{\rm r})$ and the coefficient $\lambda(r_\parallel^2)$, as well as the position of the singularity, depend on the indices ℓ, n, and the magnitude of the magnetic field $B_{\rm r}$, but the global structure of the function $I^n_{\ell\Delta}(r_\parallel^2)$ is common for any ℓ, n and $B_{\rm r}$. This is shown in Fig. 5.

Recall that the coefficients χ_i are functions of $I^n_{\ell\Delta}(r_\parallel^2)$ and thus they will show the same threshold behavior. Since χ_i are obtained after the summation over all the Landau levels specified by ℓ and $n+\ell$, and each $I^n_{\ell\Delta}(r_\parallel^2)$ has a singular point for each n and ℓ, χ_i have divergences at infinitely many thresholds. In Fig. 6, we show the real and imaginary parts

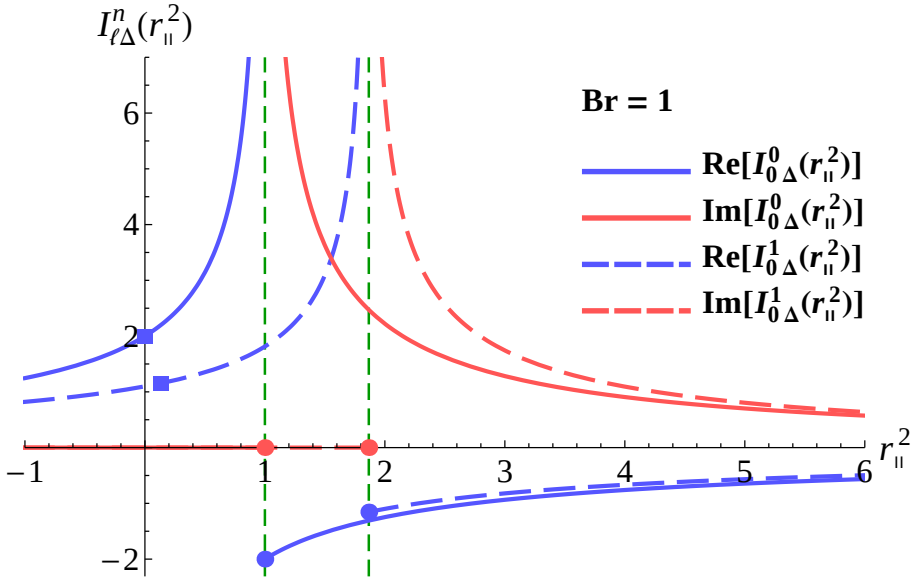

FIG. 5. The function $I^n_{\ell\Delta}(r_\parallel^2)$ is plotted against $r_\parallel^2$ for different values of n and $B_\mathrm{r} = 1$. Blue (red) solid and dashed lines are real (imaginary) parts of $I^n_{\ell\Delta}(r_\parallel^2)$ for $n = 0$ and 1, respectively. Filled squares (circles) on the lines are lower (higher) thresholds $r_\parallel^2 = s_-^{\ell n}$ ($r_\parallel^2 = s_+^{\ell n}$).

of χ_1 as functions of $r_\parallel^2$ for $B_\mathrm{r} = 10$. Among infinitely many terms, we have summed from the first term up to the 14th term. Spikes correspond to the thresholds for different values of ℓ and n. For example, the first and second thresholds appear at $r_\parallel^2 = s_+^{00} = 1$ and $r_\parallel^2 = s_+^{01} = (1 + \sqrt{1 + 2B_\mathrm{r}})^2/4 \sim 8$ for $B_\mathrm{r} = 10$. It is important to notice that these divergences are harmless in the dielectric constants $\epsilon_\perp$, $\epsilon_\parallel$ and the refractive indices $n_\perp$, $n_\parallel$. This is easily understood from the explicit representation of the dielectric constants, Eqs. (23) and (24). First, the function $I^n_{\ell\Delta}(r_\parallel^2)$ enters all the coefficients χ_i $(i = 0, 1, 2)$, and thus three of the coefficients have divergences of the same order at exactly the same momenta. Second, these coefficients appear both in the denominators and numerators of Eqs. (23) and (24). Therefore, the singularities of $I^n_{\ell\Delta}(r_\parallel^2)$ bring the same divergences in the denominators and numerators, and are canceled to give finite values of the dielectric constants and the refractive indices.

We also notice that magnitudes of the dielectric constants, in the vicinity of a threshold specified by ℓ and n, are governed by the prefactors of the terms proportional to $I^n_{\ell\Delta}(r_\parallel^2)$ in χ_i, because they dominate all the other finite terms including the terms proportional to $I^{n'}_{\ell'\Delta}(r_\parallel^2)$ with indices ℓ', n' different from ℓ, n.

(a)

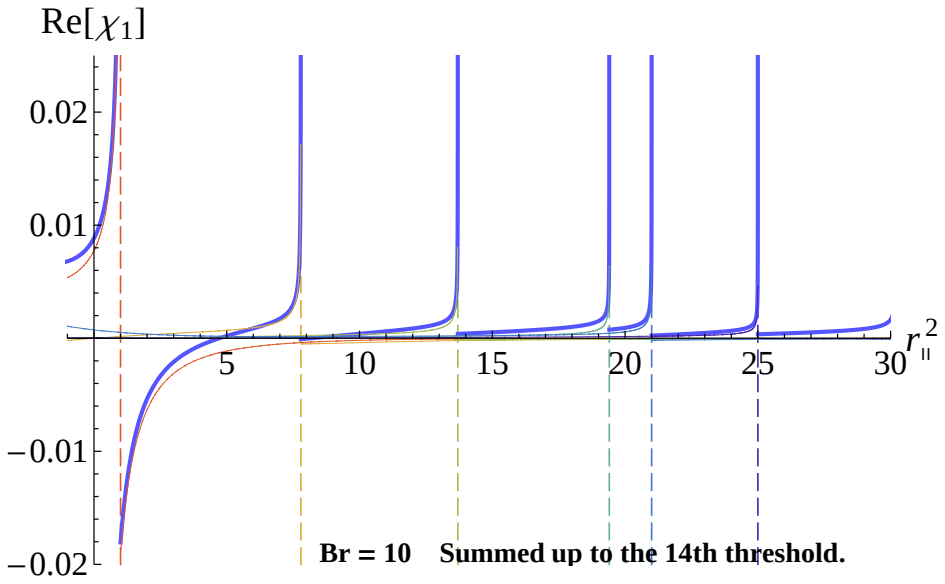

(b)

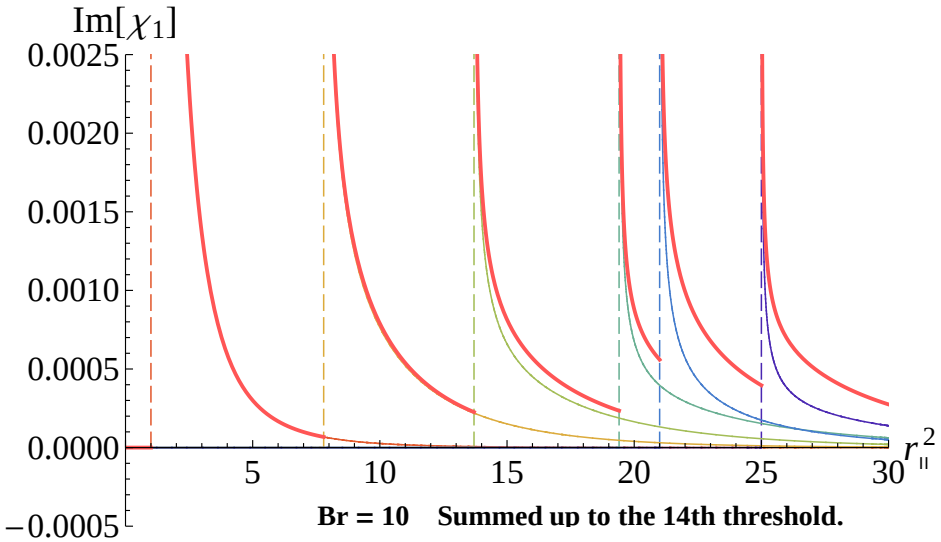

FIG. 6. Real and imaginary parts of the coefficient χ_1 as functions of $r_{\parallel}^2$ for $B_{\rm r} = 10$. Shown are the results obtained with the first 14th terms. While thin colored lines indicate individual contributions from Landau levels shown with the same colors in Fig. 4, a thick line indicates a resultant quantity after the summation.

V. SUMMARY AND PROSPECTS

In this paper, we have presented analytic representation of the vacuum polarization tensor in a strong magnetic field, which is an indispensable quantity for the description of photon's birefringence. This was made possible by the use of infinite series expansion applied to the exponentiated trigonometric functions, whose integer indices have been later physically interpreted as the Landau levels of a fermion-antifermion pair. The infinite sum corresponds to the contributions from all the Landau levels to the vacuum polarization tensor. We have carefully investigated the singularity structure of the vacuum polarization tensor at an infinite number of the thresholds beyond which a photon decays into a fermion-antifermion pair.

Having obtained the analytic expressions of the vacuum polarization tensor, we can proceed to computation of the dielectric constants $\epsilon_{\perp,\parallel}$ and refractive indices $n_{\perp,\parallel}$ by using Eqs. (23) and (24). However, this does not go straightforwardly as we have already emphasized in the last paragraph of Sec. III. We need to solve Eqs. (23) and (24) self-consistently with respect to the dielectric constants. In Ref. [18], such self-consistent solutions were numerically obtained when the photon momentum is smaller than the lowest threshold $r_\parallel^2 < 1$. The result shows that one of the refractive indices starts to deviate from unity as the magnetic field strength increases beyond the critical one $B_{\rm r} > 1$, and approaches a limiting value, depending on propagation angle, in the extremely strong field limit $B_{\rm r} \gg 1$. Our calculation of course precisely reproduces the results of Ref. [18], and can go beyond it. However, we have to be very careful when we investigate a region where the deviation of the dielectric constant becomes sizeable. In the next paper [22], we will inspect the self-consistent solutions when the photon momentum $r_\parallel^2$ increases across the threshold.

The general expression obtained in this work beyond the threshold has opened new possibilities to study a wide variety of phenomena which contain quite different scales. Recall the threshold structure shown in Fig. 4, and note that the kinematical region discussed in Ref. [18] covers a small region below the first threshold (horizontal line at $r_\parallel^2 = 1$). However, if one wants to apply to relativistic heavy-ion collision, photons generally have large momenta, and thus we have to take into account the effects of many thresholds. Also, in application to the physics in magnetars, one would be interested in the interplay and competition among photon splitting, vacuum birefringence and photon decay [31, 32]. To

investigate these intriguing phenomena, we need to accurately describe the structure of the photon spectrum with the thresholds taken into account. In the next paper [22], we will discuss how and to what extent the dielectric constants and the refractive indices are influenced by the singular behavior of the vacuum polarization tensor at the threshold. We will show that the location of the threshold itself has to be obtained in a self-consistent way. In particular, we will investigate behavior of refractive indices incorporating effects of thresholds, which can be studied within the lowest Landau level approximation.

ACKNOWLEDGEMENTS

This work was supported by Korea national research foundation under grant number KRF-2011-0030621, and also partially supported by "The Center for the Promotion of Integrated Sciences (CPIS)" of Sokendai.

Appendix A: Fermion propagator in a constant magnetic field

We describe here how to obtain the dressed fermion propagator in a constant magnetic field shown in Fig. 1. As mentioned in the text, we employ Schwinger's proper-time method [20, 21, 24], which yields the integral representation (5) with respect to the "proper-time" $\hat{\tau}$:

$$G(p|A_{\rm cl}) = i\left(\not{p} - e\not{A}_{\rm cl} + m\right) \times \frac{1}{i}\int_0^\infty d\hat{\tau}\ \mathrm{e}^{i\hat{\tau}\left\{(\not{p}-e\not{A}_{\rm cl})^2-(m^2-i\varepsilon)\right\}}\,,$$

where $A^\mu_{\rm cl}$ is the Fourier transformation of $A^\mu_{\rm cl}(x)$ and a small imaginary value $-i\varepsilon$, originated from the prescription of the boundary condition, makes the integral convergent. An advantage of this expression is that the terms containing the gauge field appear in positive powers, while in the original definition (3) the gauge field appears in the denominator. Below, we analyse the following integral part:

$$\Delta(p|A_{\rm cl}) \equiv \frac{1}{i}\int_0^\infty d\hat{\tau}\ \mathrm{e}^{i\hat{\tau}\left\{(\not{p}-e\not{A}_{\rm cl})^2-(m^2-i\varepsilon)\right\}}\quad, \tag{A1}$$

which, equivalently to Eq. (2), satisfies the following equation:

$$\left\{\left(\not{p} - e\not{A}_{\rm cl}\right)^2 - m^2\right\}\Delta(p|A_{\rm cl}) = \mathbf{1}\,. \tag{A2}$$

Note that the operator contains Dirac matrices, and thus both the equation and $\Delta(p|A_{\rm cl})$ are understood as matrices with respect to spinor indices.

It is convenient to perform calculation in the Fock-Schwinger gauge for the external field, $x_\mu A^\mu_{\rm cl}(x) = 0$, which allows one to represent the gauge field in terms of the field-strength tensor as $A^\mu(x) = -\frac{1}{2}F^{\mu\nu}x_\nu$ when the field strength is constant. An elementary calculation yields the expression for Eq. (A2) in terms of the field strength:

$$\left[p^2 - \kappa^2 + \frac{e^2}{4}\frac{\partial}{\partial p^\mu}F^{\mu\nu}F_{\nu\sigma}\frac{\partial}{\partial p_\sigma}\right]\Delta(p|A_{\rm cl}) = \mathbf{1} \quad , \tag{A3}$$

where we have introduced κ defined by

$$\kappa^2 = m^2 - i\epsilon + \frac{e}{2}F^{\mu\nu}\sigma_{\mu\nu} \, ,$$

with the antisymmetric tensor, $\sigma^{\mu\nu} = \frac{i}{2}[\gamma^\mu, \gamma^\nu]$.

By solving Eq. (A3), one can derive another expression alternative to Eq. (A1), which is favorably written with respect to the field-strength tensor. Namely, we find

$$\Delta(p|A_{\rm cl}) = \frac{1}{i}\int_0^\infty d\hat{\tau} \; \mathrm{e}^{-i\kappa^2\hat{\tau} + ip_\mu X^{\mu\nu}(\hat{\tau})p_\nu + Y(\hat{\tau})} \, , \tag{A4}$$

where we have introduced two functions $X^{\mu\nu}(\tau)$ and $Y(\tau)$ defined by

$$X^{\mu\nu}(\hat{\tau}) \equiv \left[(eF)^{-1}\tanh(eF\hat{\tau})\right]^{\mu\nu} = \hat{\tau}\;\eta_\parallel^{\mu\nu} + \frac{\tan(eB\hat{\tau})}{eB}\;\eta_\perp^{\mu\nu} \, , \tag{A5}$$

$$Y(\hat{\tau}) \equiv -\frac{1}{2}\mathrm{Tr}\left[\ln\left\{\cosh(eF\hat{\tau})\right\}\right] = -\ln|\cos(eB\hat{\tau})| \, . \tag{A6}$$

In this expression, we have suppressed contracted tensor indices, and written inverse field-strength tensor as $(F^{-1})^{\mu\nu}$. As shown above, two functions $X^{\mu\nu}(\hat{\tau})$ and $Y(\hat{\tau})$ are especially simplified when there is only a magnetic field: The field-strength tensor is then given by $F^{21} = -F^{12} = B$ with all the other elements vanishing. We find that $X^{\mu\nu}$ shows different behavior in the longitudinal ($\parallel$) and transverse ($\perp$) planes with respect to the external field, which are, respectively, specified by the metric tensors $\eta_\parallel^{\mu\nu} = \mathrm{diag}(1,0,0,-1)$ and $\eta_\perp^{\mu\nu} = \mathrm{diag}(0,-1,-1,0)$.

Substituting the above expressions (A4) – (A6) into Eqs. (5), one obtains the following integral representation of the dressed fermion propagator:

$$G(p|A_{\rm cl}) = \int_0^\infty d\hat{\tau}\Big[\not{p} - e\gamma^\mu F_{\mu\nu}X^{\nu\sigma}(\hat{\tau})p_\sigma + m\Big]\mathrm{e}^{-i\kappa^2\hat{\tau} + ip_\mu X^{\mu\nu}(\hat{\tau})p_\nu + Y(\hat{\tau})} \, . \tag{A7}$$

Recall that κ^2 contains the gamma matrices, and thus we have to take into account the order among them when we carry out the trace of spinor indices. Although integration over the proper-time $\hat{\tau}$ has not been performed, this compact form allows us to efficiently

simplify awkward expressions in applying to resummed diagram calculations which include the vacuum polarization tensor shown in Fig. 2. Owing to the Fock-Schwinger gauge, a configuration of the external field is manifestly specified in terms of the field-strength.

Appendix B: Renormalization of the vacuum polarization tensor

Below we first discuss renormalization of the polarization tensor in the ordinary vacuum, and then consider the case with the magnetic field.

Our framework for nonzero magnetic field background, of course, contains the case of the ordinary vacuum as a limit of vanishing magnetic field. This is explicitly checked in the expressions (9) – (11) which have not been expanded with respect to the Landau levels. Indeed, in a vanishing magnetic field limit $B_{\rm r} = 0$, the scalar functions χ_i $(i = 0, 1, 2)$ in Eqs. (9) – (11) reduce to the results in the ordinary vacuum. This is easily seen as follows. Since Γ_1 and Γ_2 vanish in the vanishing field limit $B_{\rm r} \to 0$ with τ and β being fixed,[14] the scalar functions χ_1 and χ_2 also vanish in this limit:

$$\chi_1 = \chi_2 = 0\,.$$

On the other hand, χ_0 reduces to the following form,

$$\chi_0^{\rm vac}(r^2) = \frac{\alpha}{4\pi}\int_{-1}^{1} d\beta \int_{\delta}^{\infty} d\tau\ \frac{1-\beta^2}{\tau}{\rm e}^{-i\phi_0\tau} \quad , \tag{B1}$$

where we have defined a phase $\phi_0(r^2) = 1-(1-\beta^2)r^2$ with a normalized squared momentum $r^2 = q^2/(4m^2)$. We have introduced a cut-off $\delta\,(0 < \delta \ll 1)$ at the lower boundary of the integral with respect to τ, because, without regularization $\delta \to 0$, there arises a logarithmic divergence in this integral. In terms of $\chi_0^{\rm vac}$, the vacuum polarization tensor in the ordinary vacuum $\Pi_0^{\mu\nu}(q^2)$, obtained as the vanishing field limit, is given by

$$\Pi_0^{\mu\nu}(q) = -\chi_0^{\rm vac}(r^2)P_0^{\mu\nu} \quad . \tag{B2}$$

When the squared momentum r^2 is less than the threshold[15], $0 < r^2 < 1$, the phase ϕ_0 becomes positive definite, and then the integral with respect to τ in Eq. (B1) is calculated as

$$\chi_0^{\rm vac} = \frac{\alpha}{4\pi}\int_{-1}^{1} d\beta(1-\beta^2)\Gamma(0, \phi_0\delta)$$

[14] One should take this limit after pulling back the proper-time τ to the original dimensionful form, $\tau \to |eB|\tau$, because the dimensionless form varies as the field-strength varies.

[15] Expression in the other range is obtained by an analytic continuation afterward, if necessary.

$$= -\frac{\alpha}{4\pi}\int_{-1}^{1} d\beta(1-\beta^2)\left\{\gamma_{\rm E} + \ln\phi_0 + \ln\delta + \mathcal{O}(\delta^1)\right\} \tag{B3}$$

where, on the first line, we have changed the contour so that we can use the 'incomplete gamma function', $\Gamma(s,t) = \int_t^\infty x^{s-1}{\rm e}^{-x}dx$, and, on the second line, we have expanded it with respect to the small cut-off scale δ. The constant $\gamma_{\rm E}$ denotes the Euler number. Note that a divergence in the limit $\delta \to 0$ is isolated from the other finite terms.

Adopting the conventional on-shell renormalization condition, we define a finite vacuum polarization tensor $\hat{\Pi}_0^{\mu\nu}(q)$ in the ordinary vacuum as,

$$\hat{\Pi}_0^{\mu\nu}(q) \equiv \Pi_0^{\mu\nu}(q) - \Pi_0^{\mu\nu}(0)\,. \tag{B4}$$

From the above on-shell condition and the expression (B3) for $\chi_0^{\rm vac}$, it is natural to introduce a finite scalar function $\hat{\chi}_0^{\rm vac}(r^2)$ by

$$\hat{\chi}_0^{\rm vac}(r^2) \equiv \chi_0^{\rm vac}(r^2) - \chi_0^{\rm vac}(0) \tag{B5}$$

$$= \frac{\alpha}{4\pi}\int_{-1}^{1} d\beta(1-\beta^2)\ln\left\{\frac{4m^2}{4m^2-(1-\beta^2)q^2}\right\}\,. \tag{B6}$$

Namely, the finite vacuum polarization tensor is given by $\hat{\chi}_0^{\rm vac}(r^2)$:

$$\hat{\Pi}_0^{\mu\nu}(q) = -\hat{\chi}_0^{\rm vac}(r^2)P_0^{\mu\nu}\,, \tag{B7}$$

which agrees with the conventional result (see, e.g, Eq. (7.91) in Ref. [23]). An integral in Eq. (B6) with respect to β is carried out analytically, and then we find an analytic form, which allows for an analytic continuation to the regimes $r^2 < 0$ and $1 < r^2$, as

$$\hat{\chi}_0^{\rm vac}(r^2) = \frac{\alpha}{3\pi}\left[\frac{1}{3} + \left(2+\frac{1}{r^2}\right)\left\{\left(\frac{1}{r^2}-1\right)^{\frac{1}{2}}\,{\rm Arccot}\left(\frac{1}{r^2}-1\right)^{\frac{1}{2}} - 1\right\}\right]\,. \tag{B8}$$

Now let us turn to the case with magnetic fields. As mentioned below Eqs. (9)-(11), the vacuum polarization tensor in the presence of the external magnetic field contains exactly the same logarithmic divergence as the one shown in Eq. (B3). Therefore, we remove the logarithmic divergence by imposing a similar on-shell renormalization condition,

$$\hat{\Pi}_{\rm ex}^{\mu\nu}(q_\parallel, q_\perp; B_{\rm r}) \equiv \Pi_{\rm ex}^{\mu\nu}(q_\parallel, q_\perp; B_{\rm r}) - \Pi_0^{\mu\nu}(q^2=0)\,, \tag{B9}$$

so that the finite vacuum polarization tensor $\hat{\Pi}_{\rm ex}^{\mu\nu}(q_\parallel, q_\perp; B_{\rm r})$ vanishes at simultaneous limits of $q_\parallel^2 = 0$, $q_\perp^2 = 0$ and $B_{\rm r} = 0$. In terms of the scalar functions χ_i, the renormalization condition is written as

$$\hat{\Pi}_{\rm ex}^{\mu\nu}(q_\parallel, q_\perp; B_{\rm r}) = -\left\{\chi_0(r_\parallel^2, r_\perp^2; B_{\rm r}) - \chi_0^{\rm vac}(0)\right\}P_0^{\mu\nu} - \sum_{i=1,2}\chi_i P_i^{\mu\nu}\,. \tag{B10}$$

To proceed further, we have to regularize the divergent scalar functions χ_0 and $\chi_0^{\rm vac}$.

We show regularization methods which are involved in our numerical [22] and analytic calculations. First, in case of numerical calculation, we regularize χ_0 and $\chi_0^{\rm vac}$ by inserting common cut-off scales into these functions. Then, the scalar function χ_0 in the presence of the external magnetic field is regularized in the same manner as in Eq. (B1),

$$\chi_0(r_\parallel^2, r_\perp^2; B_{\rm r}) = \frac{\alpha}{4\pi}\int_{-1}^{1} d\beta \int_\delta^\infty d\tau \ \frac{\Gamma_0}{\sin\tau} {\rm e}^{-i\phi\tau} \quad , \tag{B11}$$

where we have put all the phase appearing in Eq. (9) together as $\phi(r_\parallel^2, r_\perp^2) = \phi_\parallel(r_\parallel^2) + (u\cos(\beta\tau) - \eta\cos\tau)/\tau$. However, unlike the case in the ordinary vacuum (B3), a complex structure of χ_0 prevents us from isolating the divergence by an analytic calculation. We therefore numerically evaluate a convergent integral,

$$J_0(r_\parallel^2, r_\perp^2; B_{\rm r}) = \frac{\alpha}{4\pi}\int_{-1}^{1} d\beta \int_\delta^\infty d\tau \ \left[\frac{\Gamma_0(-i\tau)}{\sinh\tau}{\rm e}^{-\phi(r_\parallel^2, r_\perp^2)\tau} - \frac{1-\beta^2}{\tau}{\rm e}^{-\phi_0(0)\tau}\right] \quad , \tag{B12}$$

where we have rotated the integral contour downward in the complex τ-plane assuming a momentum regime $r_\parallel^2 < (1+\sqrt{1+2B_{\rm r}})^2/4$ so that the integrand vanishes on the large arc. We then obtain a finite part of the scalar function as,

$$\hat{\chi}_0(r_\parallel^2, r_\perp^2; B_{\rm r}) \equiv \chi_0(r_\parallel^2, r_\perp^2; B_{\rm r}) - \chi_0^{\rm vac}(0) \tag{B13}$$

$$= J_0(r_\parallel^2, r_\perp^2; B_{\rm r}) + \mathcal{R}_0(\delta) \quad . \tag{B14}$$

We have put a remainder as

$$\mathcal{R}_0(\delta) = \frac{\alpha}{4\pi}\int_{-1}^{1} d\beta \int_0^\delta d\tau \ \left[\frac{\Gamma_0(-i\tau)}{\sinh\tau}{\rm e}^{-\phi(r_\parallel^2, r_\perp^2)\tau} - \frac{1-\beta^2}{\tau}{\rm e}^{-\phi_0(0)\tau}\right] \tag{B15}$$

which gives a cut-off dependence on the right-hand side of Eq. (B14). Note that, if we could remove the cut-off scale by taking a vanishing limit $\delta \to 0$ at the end of calculation, the renormalized scalar function $\hat{\chi}_0(r_\parallel^2, r_\perp^2; B_{\rm r})$ should not depend on the cut-off scale as long as we insert common cut-off scales into χ_0 and $\chi_0^{\rm vac}$. However, we cannot take this limit in numerical calculations, and thus it should be estimated how much the renormalized scalar function $\hat{\chi}_0$ depends on the cut-off scale δ. For a small τ, the integrand is composed of the following functions,

$$\frac{\Gamma_0(-i\tau)}{\sinh\tau} \sim \frac{1-\beta^2}{\tau} + \frac{1}{6}(1-\beta^2)^2\tau + \mathcal{O}(\tau^3) \tag{B16}$$

$$\phi(r_\parallel^2, r_\perp^2) \sim \phi_0(r^2) + \mathcal{O}(\tau^3) \quad , \tag{B17}$$

and thus the remainder is evaluated as,

$$\mathcal{R}_0(\delta) \sim \frac{\alpha}{4\pi}\int_{-1}^{1}d\beta\int_0^{\delta}d\tau\ \left[-(1-\beta^2)\left\{\phi_0(r^2)-\phi_0(0)\right\}+\mathcal{O}(\tau)\right] \tag{B18}$$

$$= \frac{4\alpha}{15\pi}r^2\delta+\mathcal{O}(\delta^2)\ . \tag{B19}$$

The above estimate shows that the remainder $\mathcal{R}_0(\delta)$ is linearly suppressed as we take a small cut-off scale δ in numerical calculation.

There is an improved method to suppress the cut-off scale dependence, which we have adopted in our numerical calculation. Note that the term independent of τ in Eq. (B18) vanishes, if two phases ϕ_0 are evaluated at the same momentum. We rearrange Eq. (B13) to eliminate this constant term by using Eq. (B5) as [16]

$$\hat{\chi}_0(r_\parallel^2,r_\perp^2;B_{\rm r}) = \left\{\chi_0(r_\parallel^2,r_\perp^2;B_{\rm r})-\chi_0^{\rm vac}(r^2)\right\}+\hat{\chi}_0^{\rm vac}(r^2)\ . \tag{B20}$$

The renormalized scalar function is then obtained as,

$$\hat{\chi}_0(r_\parallel^2,r_\perp^2;B_{\rm r}) = J(r_\parallel^2,r_\perp^2;B_{\rm r})+\hat{\chi}_0^{\rm vac}(r^2)+\mathcal{R}(\delta)\ , \tag{B21}$$

with a convergent integral $J(r_\parallel^2,r_\perp^2;B_{\rm r})$ and a remainder $\mathcal{R}(\delta)$ given by

$$J(r_\parallel^2,r_\perp^2;B_{\rm r}) = \frac{\alpha}{4\pi}\int_{-1}^{1}d\beta\int_{\delta}^{\infty}d\tau\ \left[\frac{\Gamma_0(-i\tau)}{\sinh\tau}{\rm e}^{-\phi(r_\parallel^2,r_\perp^2)\tau}-\frac{1-\beta^2}{\tau}{\rm e}^{-\phi_0(r^2)\tau}\right], \tag{B22}$$

$$\mathcal{R}(\delta) = \frac{\alpha}{4\pi}\int_{-1}^{1}d\beta\int_{0}^{\delta}d\tau\ \left[\frac{\Gamma_0(-i\tau)}{\sinh\tau}{\rm e}^{-\phi(r_\parallel^2,r_\perp^2)\tau}-\frac{1-\beta^2}{\tau}{\rm e}^{-\phi_0(r^2)\tau}\right]. \tag{B23}$$

We already have an analytic expression for the renormalized scalar function $\hat{\chi}_0^{\rm vac}(r^2)$ in the ordinary vacuum. In this method, the remainder $\mathcal{R}(\delta)$ is evaluated as,

$$\mathcal{R}(\delta) \sim \frac{\alpha}{4\pi}\int_{-1}^{1}d\beta\int_0^{\delta}d\tau\ \left[\left\{\frac{1}{2}(1-\beta^2)\phi_0(r^2)-\frac{1}{6}(1-\beta^2)^2\right\}\tau+\mathcal{O}(\tau^2)\right] \tag{B24}$$

$$= \frac{\alpha}{180\pi}(11-12r^2)\delta^2+\mathcal{O}(\delta^3)\,. \tag{B25}$$

By using this method, the cut-off dependence is improved from a linear dependence $\mathcal{R}_0(\delta)\sim\mathcal{O}(\delta^1)$ to quadratic one $\mathcal{R}(\delta)\sim\mathcal{O}(\delta^2)$.

Next, we proceed to the case of our analytic calculation. In the expansion method resulting in the double infinite sum with respect to the Landau levels, we do not have to insert a cut-off scale to perform term-by-term integrals, because these contributions, from the

[16] An equivalent expression to Eq. (B20) has been shown in Ref. [19], and might be adopted to numerical computation in Ref. [18]. However, it has not been clear how it improves the naive subtraction (B13).

discretized levels in the transverse momentum, does not diverge individually. However, by taking all-order summation, we show that the infinite sum leads to a logarithmic divergence which should be identified with the logarithmic divergence we have seen above.

We examine the double infinite series at vanishing momenta $r_\parallel^2 = 0$ and $r_\perp^2 = 0$, because the ultraviolet divergence itself does not depend on external momentum scales. At these momenta, the series coefficient C_ℓ^n and its multiplicative form in χ_0 have simple expressions,

$$C_\ell^n(0) = \begin{cases} 1 & (n=0) \\ 0 & (n \geq 1) \end{cases} \tag{B26}$$

$$\frac{n}{\eta} C_\ell^n(0) = \begin{cases} \ell+1 & (n=1) \\ 0 & (n \geq 2) \end{cases} , \tag{B27}$$

where we have used $L_\ell^0(0) = 1$ and $L_\ell^1(0) = \ell + 1$. Note that the expression of χ_0 should be understood that any term being proportional to $n/\eta \times C_\ell^n(0)$ at $n = 0$ is absent, because such term never exists in the expansion (E3). Then, summation of the coefficients in χ_2 (see Eqs. (43) and (44)) are also easily performed as

$$D_\ell^{0(1)}(0) = -8 \sum_{\lambda=0}^{\ell-1} (\ell - \lambda) \left\{ -C_\ell^0(0) \right\} = 4\ell(\ell+1) \ , \tag{B28}$$

$$D_\ell^{1(1)}(0) = -8 \sum_{\lambda=0}^{\ell-1} (\ell - \lambda) C_\ell^0(0) = -4\ell(\ell+1) \ , \tag{B29}$$

$$D_\ell^{2(1)}(0) = -8 \sum_{\lambda=0}^{\ell-2} (\ell - \lambda - 1) \left\{ -C_\ell^0(0) \right\} = 4\ell(\ell-1) \ . \tag{B30}$$

Therefore, the infinite series with respect to n terminates up to the first two terms. At vanishing momenta and for $n = 0, 1$, the functions $F_\ell^n(0)$, $G_\ell^n(0)$ and $H_\ell^n(0)$ have the following forms:

$$F_\ell^0(0) = \frac{2}{1 + 2\ell B_{\rm r}} , \tag{B31}$$

$$F_\ell^1(0) = -\frac{1}{B_{\rm r}} \Xi_\ell^1 , \tag{B32}$$

$$G_\ell^1(0) = -\frac{1}{B_{\rm r}^2} \left[\{1 + (2\ell+1) B_{\rm r}\} \Xi_\ell^1 + 2B_{\rm r} \right] , \tag{B33}$$

$$H_\ell^0(0) = \frac{2}{3} \cdot \frac{1}{1 + 2\ell B_{\rm r}} . \tag{B34}$$

By using these explicit expressions, we show that the scalar coefficient χ_0 and differences $\chi_1 - \chi_0$ and $\chi_2 - \chi_0$ contain the same logarithmic divergence. Introducing $\tilde{\chi}_i = \chi_i - (1 - \delta_{i0})\chi_0$,

we have

$$\tilde{\chi}_i(r_\parallel^2 = r_\perp^2 = 0; B_{\rm r}) = \frac{\alpha B_{\rm r}}{4\pi}\left\{u_i(B_{\rm r}) + \sum_{\ell=1}^{\infty} w_i(\ell; B_{\rm r})\right\} \quad , \tag{B35}$$

where we separated an infinite series with respect to ℓ so that it begins from $\ell = 1$. Explicit expressions of terms are given by

$$u_i(B_{\rm r}) = \begin{cases} 2\,(F_0^1 - G_0^1) & (i=0) \\ F_0^0 + F_1^0 - (H_0^0 + H_1^0) & (i=1) \\ 0 & (i=2) \end{cases} \tag{B36}$$

and

$$w_i(\ell; B_{\rm r}) = \begin{cases} 2\left\{F_\ell^1 - (2\ell+1)G_\ell^1\right\} & (i=0) \\ F_\ell^0 + F_{\ell+1}^0 - (H_\ell^0 + H_{\ell+1}^0) & (i=1) \\ 4\ell(\ell+1)\left\{(F_\ell^0 - 2F_\ell^1) + F_{\ell+1}^0\right\} & (i=2) \end{cases} \quad . \tag{B37}$$

Here, we suppressed the vanishing arguments of $F_\ell^n(0)$, $G_\ell^n(0)$ and $H_\ell^n(0)$. To see a behavior of the summation taken up to a large ℓ, we insert a cut-off at $\ell = L$ assuming an infinite limit $L \to \infty$. The infinite sum is then evaluated by being replaced by an integral as,

$$\begin{aligned} \tilde{\chi}_i(r_\parallel^2 = r_\perp^2 = 0; B_{\rm r}) &= \frac{\alpha B_{\rm r}}{4\pi}\left\{u_i(B_{\rm r}) + \lim_{L\to\infty} L\sum_{\ell=1}^{L}\frac{1}{L} w_i(\ell; B_{\rm r})\right\} \\ &= \frac{\alpha B_{\rm r}}{4\pi}\left\{u_i(B_{\rm r}) + \lim_{L\to\infty} L\int_0^1 dx\, w_i(Lx; B_{\rm r})\right\} \quad . \end{aligned} \tag{B38}$$

The above integrals are carried out analytically, and then expanded for a large value of L as,

$$\tilde{\chi}_i(r_\parallel^2 = r_\perp^2 = 0; B_{\rm r}) = \frac{\alpha}{3\pi}\ln(2B_{\rm r}L) + \sum_{k=0}^{\infty} c_k(B_{\rm r}) L^{-k} \quad , \tag{B39}$$

where series coefficients are denoted by $c_k(B_{\rm r})$. The above expansion series does not have any positive power of L, and thus the leading term for large L (with finite $B_{\rm r}$) is given by a divergent logarithm. Note also that a coefficient of the divergent term is independent of $B_{\rm r}$, implying the same divergence as in the ordinary vacuum. While the scalar functions χ_1 and χ_2 do not contain any divergence owing to a cancellation between the logarithmic terms in the functions $\tilde{\chi}_i$, the other one χ_0 contains the logarithmic divergence found in Eq. (B39). These results are consistent with the observation below Eq. (9) – (11). Therefore, we might be allowed to identify this divergent logarithm, appearing from the infinite sum, with the one

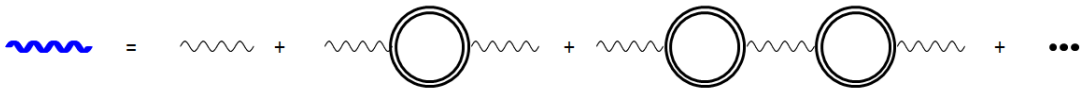

FIG. 7. A modified photon propagator

in Eq. (B3) appearing in the limit $\delta \to 0$. Comparing them up to the divergent logarithmic term as

$$\frac{\alpha}{3\pi}\ln(\delta^{-1}) = \frac{\alpha}{3\pi}\ln(2B_{\rm r}L) \quad , \tag{B40}$$

we then find a relation between the cut-off scales,

$$\delta^{-1} = 2B_{\rm r}L \quad . \tag{B41}$$

According to this relation (B41), the ultraviolet logarithmic divergence in the presence of a magnetic field is subtracted by the same logarithmic divergence in the ordinary vacuum. Namely, the divergent contribution in a sum up to $\ell = L \gg 1$ might require to be subtracted by an integral (B1) evaluated with a cut-off scale $\delta = (2B_{\rm r}L)^{-1}$, and a finite part in our prescription is defined as a remainder of this subtraction.

Appendix C: Dispersion relations from modified photon propagator

Here we demonstrate that one can obtain Eq. (21) (that immediately yields the dispersion relations (23) and (24)) from pole positions of a modified photon propagator after taking into account the interactions with the external magnetic field.

First of all, it should be noticed that insersion of the self-energy $\Pi^{\mu\nu}_{\rm ex}$ into a photon propagator corresponds to resumming the dressed-fermion one-loop diagrams as shown in Fig. 7. There, the dressed-fermion one-loops are linked by the free photon propagators $D^{\mu\nu}_0(q^2)$ given by

$$iD^{\mu\nu}_0(q) \equiv \frac{1}{q^2}\left[\eta^{\mu\nu} - (1-\xi_g)\frac{q^\mu q^\nu}{q^2}\right] . \tag{C1}$$

A full photon propagator in this approximation can be expressed as

$$D^{\mu\nu}(q) = \sum_{n=0}^{\infty} D^{\mu\nu}_n(q)\,, \tag{C2}$$

where the n-th contribution corresponds to the diagram having n rings, and $n = 0$ is the free propagator $D_0^{\mu\nu}$. To compute the n-th order contribution $D_n^{\mu\nu}(q^2)$, we use the following identities among the projection operators $P_i^{\mu\nu}$:

$$
\begin{aligned}
&P_0^{\mu\rho} P_{i\rho}{}^{\nu} = P_i^{\mu\rho} P_{0\rho}{}^{\nu} = q^2 P_i^{\mu\nu} \quad (i = 0, 1, 2)\,, \\
&P_1^{\mu\rho} P_{1\rho}{}^{\nu} = q_\parallel^2 P_1^{\mu\nu}\ , \quad P_2^{\mu\rho} P_{2\rho}{}^{\nu} = q_\perp^2 P_2^{\mu\nu}\ , \quad P_1^{\mu\rho} P_{2\rho}{}^{\nu} = P_2^{\mu\rho} P_{1\rho}{}^{\nu} = 0 \ . \qquad \text{(C3)}
\end{aligned}
$$

Since, as shown by the above relations, the products of two projection operators always result in zero or one of the projection operators, we are able to expand the n-th order diagram into the same form as the self-energy with respect to the projection operators:

$$
\begin{aligned}
D_n^{\mu\nu}(q) &= D_0^{\mu\rho_1}(i\Pi_{\mathrm{ex}\rho_1\sigma_1} D_0^{\sigma_1\rho_2}) \cdots (i\Pi_{\mathrm{ex}\rho_n\sigma_n} D_0^{\sigma_n\nu}) \\
&\equiv \zeta_0^{(n)} P_0^{\mu\nu} + \zeta_1^{(n)} P_1^{\mu\nu} + \zeta_2^{(n)} P_2^{\mu\nu} \ . \qquad \text{(C4)}
\end{aligned}
$$

For $n \geq 1$, we can drop those terms proportional to $q^\mu q^\nu$ in the free propagator (C1), because they vanish when contracted with any of the projection operators in the self-energy as $q_\mu P_i^{\mu\nu} = 0$ $(i = 0, 1, 2)$. The coefficient scalar functions are then calculated as

$$
\begin{aligned}
\zeta_0^{(n)} &= \left(\frac{-i}{q^2}\right) \times \left(-\frac{\chi_0}{q^2}\right)^n (q^2)^{n-1}\,, \qquad \text{(C5)} \\
\zeta_1^{(n)} &= \left(\frac{-i}{q^2}\right) \times \sum_{r=0}^{n-1} {}_n\mathrm{C}_r \left(-\frac{\chi_0}{q^2}\right)^r \left(-\frac{\chi_1}{q^2}\right)^{n-r} (q^2)^r \ (q_\parallel^2)^{n-1-r} \\
&= \left(\frac{-i}{q^2}\right) \times \frac{(-1)^n}{q_\parallel^2} \left\{ \left(\chi_0 + \frac{q_\parallel^2}{q^2}\chi_1\right)^n - (\chi_0)^n \right\}\,, \qquad \text{(C6)} \\
\zeta_2^{(n)} &= \zeta_1^{(n)}\,(1 \to 2\ ,\ \ \parallel \to \perp)\ , \qquad \text{(C7)}
\end{aligned}
$$

where the last line is meant for replacements of subscripts in $\zeta_1^{(n)}$ as indicated. To carry out the summations in $\zeta_1^{(n)}$ and $\zeta_2^{(n)}$, we used a formula for the binomial expansion. Substituting Eq. (C4) with the coefficients (C5) – (C7) into Eq. (C2), we obtain the resummed photon propagator as

$$
\begin{aligned}
&iD^{\mu\nu}(q) \\
&= \frac{1}{(1+\chi_0)q^2} \cdot \frac{P_0^{\mu\nu}}{q^2} + \frac{\sigma_\parallel(q^2, q_\parallel^2)}{(1+\chi_0)q^2 + \chi_1 q_\parallel^2} \cdot \frac{P_1^{\mu\nu}}{q_\parallel^2} + \frac{\sigma_\perp(q^2, q_\perp^2)}{(1+\chi_0)q^2 + \chi_2 q_\perp^2} \cdot \frac{P_2^{\mu\nu}}{q_\perp^2} + \frac{\xi_g}{q^2} \cdot \frac{q^\mu q^\nu}{q^2} \\
&= \frac{\pi_{(0)}^\mu \pi_{(0)}^\nu}{(1+\chi_0)q^2} + \frac{\pi_{(1)}^\mu \pi_{(1)}^\nu}{(1+\chi_0)q^2 + \chi_2 q_\perp^2} + \frac{\pi_{(2)}^\mu \pi_{(2)}^\nu}{(1+\chi_0)q^2 + \chi_1 q_\parallel^2} + \frac{\xi_g}{q^2} \pi_{(3)}^\mu \pi_{(3)}^\nu\,. \qquad \text{(C8)}
\end{aligned}
$$

We have introduced $\sigma_{\parallel}(q^2, q_{\parallel}^2) \equiv -q_{\parallel}^2\chi_1/\{q^2(1+\chi_0)\}$ and $\sigma_{\perp}(q^2, q_{\perp}^2) \equiv -q_{\perp}^2\chi_2/\{q^2(1+\chi_0)\}$, and utilized relations shown in Eq. (17) to get a 'diagonalized' form on the second line. Contracting the propagator (C8) with eigenvectors as, $\pi_{(i)}^{\mu} D_{\mu\nu} \pi_{(i)}^{\nu}$ $(i = 0, 1, 2, 3)$, we find that the pole position of each mode exactly agrees with what has been obtained in Eq. (21) from diagonalization of the modified Maxwell equation.

Appendix D: Physical modes of a photon in a magnetic field

In this Appendix, we show that, among four polarization modes in Eq. (21), only two modes, having nontrivial dispersions, are physical. We consider electric and magnetic fields of the dynamical photon field (20) whose polarizations are specified by the eigenvectors $\pi_{(\lambda)}^{\mu}$ $(\lambda = 0, \cdots, 3)$ defined in Eq. (19). Explicitly, the Fourier modes of the electric field $\mathcal{E}^i \equiv -F^{0i}$ and magnetic field $\mathcal{B}^i \equiv \frac{1}{2}\epsilon^{ijk}F_{jk}$ of a propagating photon a^{μ} in Eq. (20) are, respectively, given by

$$\mathcal{E}_{(\lambda)}^{i}(q) = iN\left(\omega\pi_{(\lambda)}^{i} - q^i\pi_{(\lambda)}^{0}\right) \mathrm{e}^{-i(\omega t - \boldsymbol{q}\cdot\boldsymbol{x})}\,, \tag{D1}$$

$$\mathcal{B}_{(\lambda)}^{i}(q) = iN\left(\epsilon^{ijk}q^j\pi_{(\lambda)}^{k}\right) \mathrm{e}^{-i(\omega t - \boldsymbol{q}\cdot\boldsymbol{x})}\,. \tag{D2}$$

Let us first consider the polarization modes $\lambda = 0$ and 3 (see Eq. (16)), both of which give the ordinary dispersion relation of the massless type $\omega^2 = |\boldsymbol{q}^2|$. Substituting the definitions of $\pi_{(0)}^{\mu}$ and $\pi_{(3)}^{\mu}$ into the above, one immediately finds

$$\vec{\mathcal{E}}_{(0)} \propto \begin{pmatrix} q_x \\ q_y \\ 0 \end{pmatrix} q^2 = \vec{0}\,, \qquad \vec{\mathcal{B}}_{(0)} \propto \begin{pmatrix} q_y \\ -q_x \\ 0 \end{pmatrix} q^2 = \vec{0}\,, \quad \text{for } \lambda = 0\,, \tag{D3}$$

and

$$\vec{\mathcal{E}}_{(3)} = \vec{0}\,, \qquad \vec{\mathcal{B}}_{(3)} = \vec{0}\,, \quad \text{for } \lambda = 3\,, \tag{D4}$$

where the dispersion relation $q^2 = 0$ has been used for the $\lambda = 0$ mode. Namely, the two modes $\lambda = 0, 3$ do not induce excitation of the electromagnetic fields, which implies that they are unphysical. In fact, these modes are related to redundant gauge degrees of freedom.

In contrast, the remaining two modes $\lambda = 1, 2$ provide nonvanishing electromagnetic fields. First of all, one can easily verify (without using the dispersion relations) that the electric field and the magnetic field are orthogonal to each other for each mode: $\vec{\mathcal{E}}_{(\lambda)} \cdot \vec{\mathcal{B}}_{(\lambda)} =$

0 ($\lambda = 1, 2$). Next, let us employ the same coordinates as those used in deriving Eqs. (23) and (24). Then the electromagnetic field of the $\lambda = 1$ mode (with momentum q^μ) reads

$$\vec{\mathcal{E}}_{(1)}(t, \boldsymbol{x}) = \omega N \begin{pmatrix} 0 \\ 1 \\ 0 \end{pmatrix} \Psi_\perp(t, \boldsymbol{x}) \,, \quad \vec{\mathcal{B}}_{(1)}(t, \boldsymbol{x}) = \omega N \begin{pmatrix} \cos\theta \\ 0 \\ \sin\theta \end{pmatrix} \Psi_\perp(t, \boldsymbol{x}) \quad , \tag{D5}$$

where the common factor $\Psi_\perp(t, \boldsymbol{x})$ is defined by

$$\Psi_\perp(t, \boldsymbol{x}) \equiv \exp\big\{ -i\omega(t - n_\perp^{\rm real}\, \hat{\boldsymbol{q}} \cdot \boldsymbol{x})\big\} \exp\big\{ -\omega n_\perp^{\rm imag}\, \hat{\boldsymbol{q}} \cdot \boldsymbol{x}\big\} \,. \tag{D6}$$

Note that the factor includes real and imaginary parts of the refractive index $n_\perp$, which respectively represent oscillation and decay behavior of the electromagnetic field. Thus, they give a phase velocity and damping coefficient, respectively. A unit vector $\hat{\boldsymbol{q}}$ denotes a three-dimensional vector directed in the photon momentum $\boldsymbol{q}$. As in a photon in the ordinary vacuum, these fields are transverse to the photon momentum: $\vec{q} \cdot \vec{\mathcal{E}}_{(1)} = \vec{q} \cdot \vec{\mathcal{B}}_{(1)} = 0$. The electric field induced in this mode is oriented to the transverse direction with respect to the external magnetic field, and thus does not have parallel component.

Similarly, the electromagnetic field of the last remaining mode $\lambda = 2$ is given by

$$\vec{\mathcal{E}}_{(2)} = \omega N \sqrt{\frac{\epsilon_\parallel(\theta)}{\epsilon_\parallel(\frac{\pi}{2})}} \begin{pmatrix} \epsilon_\parallel\big(\frac{\pi}{2}\big)\cos\theta \\ 0 \\ \sin\theta \end{pmatrix} \Psi_\parallel(t, \boldsymbol{x}) \,, \quad \vec{\mathcal{B}}_{(2)} = \omega N \sqrt{\epsilon_\parallel\Big(\frac{\pi}{2}\Big)} \begin{pmatrix} 0 \\ -1 \\ 0 \end{pmatrix} \Psi_\parallel(t, \boldsymbol{x}) \,. \tag{D7}$$

where $\epsilon_\parallel(\theta)$ denotes the dielectric constant when the photon momentum is directed to the zenith angle θ. While the magnetic field is transverse to the photon momentum $\vec{q} \cdot \vec{\mathcal{B}}_{(2)} = 0$, we notice that the electric field in general has an overlap with the photon momentum as, $\vec{q} \cdot \vec{\mathcal{E}}_{(2)} = \omega N \sqrt{\frac{\epsilon_\parallel(\theta)}{\epsilon_\parallel(\frac{\pi}{2})}} \big\{\epsilon_\parallel\big(\frac{\pi}{2}\big) - 1\big\} \sin\theta\cos\theta$, depending on the propagation angle θ with respect to the external magnetic field.

The space-time dependence of the field is again represented by a common factor $\Psi_\parallel(t, \boldsymbol{x})$, and it describes oscillation and decay behavior of the field. However, it contains the refractive index $n_\parallel$ (instead of $n_\perp$). Namely, the factor is explicitly written as

$$\Psi_\parallel(t, \boldsymbol{x}) \equiv \exp\big\{ -i\omega(t - n_\parallel^{\rm real}\, \hat{\boldsymbol{q}} \cdot \boldsymbol{x})\big\} \exp\big\{ -\omega n_\parallel^{\rm imag}\, \hat{\boldsymbol{q}} \cdot \boldsymbol{x}\big\}. \tag{D8}$$

Recall that the refractive index $n_\parallel$ is in general different from $n_\perp$ in $\Psi_\perp(t, \boldsymbol{x})$. Therefore, the two physical modes $\lambda = 1, 2$ have distinct phase velocities and decay rates (into a fermion-antifermion pair). The electric field shown in Eq. (D7) contains a component oscillating

along the external field in which direction a charged particle has continuous spectrum. This is in contrast to the electric field of the other physical mode. Since the external magnetic field provides anisotropic spectra of fermions in the Dirac sea, oscillating electric fields, $\vec{\mathcal{E}}_{(1)}$ and $\vec{\mathcal{E}}_{(2)}$, of an incident photon induce anisotropic polarizations.

Appendix E: Partial wave decomposition

We expand exponentiated trigonometric functions in Eqs. (9) – (11) by using the Jacobi-Anger expansion that is well-known as the partial-wave decomposition [26]:

$$\begin{aligned}
\exp\{-iu\cos(\beta\tau)\} &= \sum_{n=0}^{\infty}(2-\delta_{n0})(-i)^n J_n(u)\cos(n\beta\tau) \\
&= \sum_{n=0}^{\infty}(2-\delta_{n0}) I_n(-iu)\cos(n\beta\tau) \\
&\to \sum_{n=0}^{\infty}(2-\delta_{n0}) I_n(-iu)\ \mathrm{e}^{in\beta\tau}\,, \qquad \text{(E1)} \\
\cos(\beta\tau)\exp\{-iu\cos(\beta\tau)\} &= i\frac{\partial}{\partial u}\exp\{-iu\cos(\beta\tau)\} \\
&= \sum_{n=0}^{\infty}\frac{1}{2}(2-\delta_{n0})\left\{I_{n+1}(-iu)+I_{n-1}(-iu)\right\}\cos(n\beta\tau) \\
&\to \sum_{n=0}^{\infty}\frac{1}{2}(2-\delta_{n0})\left\{I_{n+1}(-iu)+I_{n-1}(-iu)\right\}\ \mathrm{e}^{in\beta\tau}\,, \qquad \text{(E2)} \\
\sin(\beta\tau)\exp\{-iu\cos(\beta\tau)\} &= \frac{1}{iu\beta}\frac{\partial}{\partial\tau}\exp\{-iu\cos(\beta\tau)\} \\
&= \frac{i}{u}\sum_{n=0}^{\infty} n(2-\delta_{n0}) I_n(-iu)\sin(n\beta\tau) \\
&\to \frac{1}{u}\sum_{n=0}^{\infty} n(2-\delta_{n0}) I_n(-iu)\ \mathrm{e}^{in\beta\tau}\,, \qquad \text{(E3)}
\end{aligned}$$

where $J_n(z)$ and $I_n(z)$ are the Bessel and modified Bessel functions of the first kind related as, $I_n(z) = (-i)^n J_n(iz)$. Noting that the integrands in Eq. (29) are even function of β, we have replaced the trigonometric functions by exponential factors on the right-hand sides of the arrows, i.e., $\cos(n\beta\tau) \to \mathrm{e}^{in\beta\tau}$ and $\sin(n\beta\tau) \to -i\mathrm{e}^{in\beta\tau}$.

Appendix F: Limiting form of the coefficient $C_\ell^n(\eta)$

An approximate form of $C_\ell^n(\eta)$ for large values of $\ell \gg 1$ is found by the use of a limiting form of the associated Laguerre polynomial and Stirling's formula for the factorial $\ell!$. When ℓ is large enough with fixed n and η, a limiting form of the associated Laguerre polynomial $L_\ell^n(\eta)$ is expressed as (see (13.5.14) in Ref. [33]),

$$L_\ell^n(\eta) \sim \frac{1}{\sqrt{\pi\ell}} \left(\frac{\ell}{\eta}\right)^{\frac{n}{2}+\frac{1}{4}} \mathrm{e}^{\frac{\eta}{2}} \cos\Psi_\ell^n(\eta)\,, \tag{F1}$$

$$\Psi_\ell^n(\eta) = 2\sqrt{\eta\left(\ell + \frac{n+1}{2}\right)} - \frac{\pi}{2}\left(n+\frac{1}{2}\right)\,. \tag{F2}$$

Also, we use Stirling's formula for large ℓ (see (6.1.38) in Ref. [33]),

$$\ell! \sim \sqrt{2\pi}\,\mathrm{e}^{-\ell}\,\ell^{\ell+\frac{1}{2}}\quad. \tag{F3}$$

Then, the ratio of factorials in $C_\ell^n(\eta)$ for large $\ell \gg 1$ reads,

$$\begin{aligned}\frac{\ell!}{(\ell+n)!} &\sim \mathrm{e}^n \ell^{-n} \left(\frac{\ell}{\ell+n}\right)^{\ell+n+\frac{1}{2}} \\ &\sim \mathrm{e}^{-\frac{n+1}{2\ell}} \ell^{-n}\quad,\end{aligned} \tag{F4}$$

where we have used $\{\ell/(\ell+n)\}^{\ell+n+1/2} = \mathrm{e}^{-(\ell+n+1/2)\ln(1+n/\ell)} \sim \mathrm{e}^{-n\{1+(n+1)/(2\ell)\}}$ to obtain the final expression. By using Eqs. (F1), (F2) and (F4), we find a limiting form of $C_\ell^n(\eta)$ as,

$$C_\ell^n(\eta) \sim \frac{1}{\pi\sqrt{\eta\ell}}\,\mathrm{e}^{-\frac{n+1}{2\ell}} \cos^2\Psi_\ell^n(\eta) \qquad (\ell \gg 1)\,. \tag{F5}$$

The amplitude of $C_\ell^n(\eta)$ is bounded by a prefactor of the squared cosine which decays by an inverse-square-root as ℓ becomes large (see Fig. 3).

Appendix G: Imaginary part of the function $I_{\ell\Delta}^n(r_\parallel^2)$

In this Appendix, we carefully investigate analytic properties of the function $I_{\ell\Delta}^n(r_\parallel^2) = I_{\ell+}^n(r_\parallel^2) - I_{\ell-}^n(r_\parallel^2)$ (see Eq. (35)) which is the only one possible source of the imaginary contribution and thus determines the essential behavior of the vacuum polarization tensor. In the following, we consider the function $I_{\ell\Delta}^n(r_\parallel^2)$ with the indices ℓ and n being fixed.

As mentioned in the text, the property of $I_{\ell\Delta}^n(r_\parallel^2)$ is specified by the discriminant $\mathcal{D}$ defined by Eq. (46). Using the solutions $r_\parallel^2 = s_\pm^{\ell n}$ to the equation $\mathcal{D} = 0$ (see Eq. (47)), we

consider three kinematical regions (for notational simplicity, we suppress the indices ℓ and n in $s_\pm^{\ell n}$):

$$\begin{aligned} &\text{(I)} && r_\parallel^2 < s_- && (\mathcal{D} < 0) \\ &\text{(II)} && s_- < r_\parallel^2 < s_+ && (\mathcal{D} > 0) \\ &\text{(III)} && s_+ < r_\parallel^2 && (\mathcal{D} < 0)\,. \end{aligned} \tag{G1}$$

In region (II) where $\mathcal{D} > 0$, $I^n_{\ell\Delta}(r_\parallel^2)$ is obviously a real-valued function of $r_\parallel^2$, and thus there arises no imaginary part. In regions (I) and (III), the argument of the cotangent in $I^n_{\ell\pm}(r_\parallel^2)$ becomes a pure imaginary number. The expression of $I^n_{\ell\pm}(r_\parallel^2)$ in these regions is available via analytic continuation of the function in region (I). With an infinitesimal imaginary displacement $r_\parallel^2 + i\epsilon$, analytic continuation into the regions (I) and (III) leads to the following form valid in both regions:

$$\begin{aligned} I^n_{\ell\pm}(r_\parallel^2 + i\epsilon) &= \frac{-2i}{\sqrt{b^2 - 4ac}} \arctan\left\{-i(w_\pm + i\epsilon\kappa_\pm)\right\} \\ &= \frac{1}{\sqrt{b^2 - 4ac}} \left\{\ln(1 - w_\pm - i\epsilon\kappa_\pm) - \ln(1 + w_\pm + i\epsilon\kappa_\pm)\right\} \end{aligned} \tag{G2}$$

where we have introduced two real-valued functions, $w_\pm(r_\parallel^2) = (b \pm 2a)/\sqrt{b^2 - 4ac}$ and $\kappa_\pm(r_\parallel^2) = b \mp 2a$. The latter functions $\kappa_\pm$ are leading-order coefficients in an expansion of $w_\pm(r_\parallel^2 + i\epsilon)$ with respect to the infinitesimal displacement. Owing to the expression in terms of the logarithm, we notice that the arctangent has an imaginary part when the absolute values of $w_\pm$ are larger than one, $|w_\pm| > 1$, and that its sign can be either positive or negative depending on the sign of $\kappa_\pm$.

First, we show in what region $I^n_{\ell\pm}(r_\parallel^2)$ has an imaginary part. Comparing the denominator and numerator of $w_\pm$ as $(b \pm 2a)^2 - \sqrt{b^2 - 4ac}^2 = 4r_\parallel^2\{1 + (2\ell + n \mp n)B_{\rm r}\}$, we obtain inequalities $|w_\pm| > 1$ and $|w_\pm| \le 1$, when the longitudinal momentum squared is positive $r_\parallel^2 > 0$ and negative $r_\parallel^2 \le 0$, respectively. Therefore, $I^n_{\ell\pm}(r_\parallel^2)$ has an imaginary part only in the positive regime, $r_\parallel^2 > 0$.

Next, we should notice that the difference $I^n_{\ell\Delta}(r_\parallel^2) = I^n_{\ell+}(r_\parallel^2) - I^n_{\ell-}(r_\parallel^2)$ has an imaginary part only when the functions $I^n_{\ell\pm}(r_\parallel^2)$ have imaginary parts with opposite signs: otherwise, they cancel each other. The difference $I^n_{\ell\Delta}(r_\parallel^2)$ retains an imaginary part when the arguments of the arctangent, $w_\pm + i\kappa_\pm$, are on the opposite sides of the branch cut. Thus, we shall examine the signs of $w_\pm$ and $\kappa_\pm$ in more detail, which simply follow from those of $b + 2a$ and $b - 2a$ according to their definition below Eq. (G2).

In the following, the signs of the arguments are found in the regions, $0 < r_\parallel^2 < s_-$ and $s_+ < r_\parallel^2$ $(0 \le s_- < s_+)$, separately. First, we find an obvious inequality, $b - 2a = -(nB_{\rm r} + 2r_\parallel^2) < 0$, as long as $r_\parallel^2 > 0$. Thus, the signs of $\mathrm{sgn}(w_-)$ and $\mathrm{sgn}(\kappa_+)$ immediately follows in the both regions as

$$\mathrm{sgn}(w_-) < 0 \ \text{ and } \ \mathrm{sgn}(\kappa_+) < 0 \quad (0 < r_\parallel^2) \ . \tag{G3}$$

On the other hand, the signs of the other functions depend on the momentum regime. To see this, we show two relevant inequalities valid in the each regime,

$$b + 2a < -nB_{\rm r} + 2s_- < (1 + 2\ell B_{\rm r}) - \sqrt{1 + 2\ell B_{\rm r}}^2 = 0 \quad (0 < r_\parallel^2 \le s_-) \ , \tag{G4}$$

$$b + 2a > -nB_{\rm r} + 2s_+ > -nB_{\rm r} + \frac{1}{2}\sqrt{1 + 2(\ell + n)B_{\rm r}}^2 > 0 \quad (s_+ \le r_\parallel^2) \ . \tag{G5}$$

Led by these inequalities, we obtain the signs of the remaining two functions depending on the regime:

$$\mathrm{sgn}(w_+) < 0 \ \text{ and } \ \mathrm{sgn}(\kappa_-) < 0 \quad (0 < r_\parallel^2 < s_-) \ , \tag{G6}$$

$$\mathrm{sgn}(w_+) > 0 \ \text{ and } \ \mathrm{sgn}(\kappa_-) > 0 \quad (s_+ < r_\parallel^2) \ . \tag{G7}$$

Remind that the branch cut of the arctangent is located on the imaginary axis. From Eqs. (G3) and (G6), we find that the imaginary parts of $I^n_{\ell\pm}(r_\parallel^2)$ have the same signs in the regime $0 < r_\parallel^2 < s_-$, and that the function $I^n_{\ell\Delta}(r_\parallel^2)$ does not have any imaginary part in this regime. On the other hand, from Eqs. (G3) and (G7), we find that the imaginary parts of $I^n_{\ell\pm}(r_\parallel^2)$ have the opposite signs in the regime $s_+ < r_\parallel^2$, and that the function $I^n_{\ell\Delta}(r_\parallel^2)$ has an imaginary part in this regime. Therefore, we conclude that the difference $I^n_{\ell\Delta}(r_\parallel^2)$ retains an imaginary part only in the regime $s_+ < r_\parallel^2$, namely, in region (III). A piecewise representation of $I^n_{\ell\Delta}(r_\parallel^2)$ is shown in Eq. (48). It has the same form for the real part in regions (I) and (III), but has an imaginary part only in region (III).

The imaginary part in the regime $s_+^{\ell n} < r_\parallel^2$ is related to the analytic property of the vacuum polarization tensor in the complex $r_\parallel^2$-plane. It reflects that there are an infinite number of branch cuts initiating at the thresholds of photon decay, $r_\parallel^2 = s_+^{\ell n}$, specified by pairs of Landau-level indices ℓ and $\ell + n$, where a created fermion and antifermion pair has vanishing longitudinal momenta along the external magnetic field. Because the longitudinal momenta of a created fermion pair is continuous, each branch cut run continuously along the real axis into the asymptotic regime, $r_\parallel^2 \to \infty$.

Appendix H: Limiting behavior of $I^n_{\ell\Delta}(r^2_\parallel)$ at the boundaries

In this Appendix, we discuss the limiting behavior of $I^n_{\ell\Delta}(r^2_\parallel)$ in Eq. (48) at the boundaries, $r^2_\parallel = s_\pm$ (we suppress the indices ℓ and n for simplicity). We put a square root of the discriminant as $\delta = \sqrt{|b^2 - 4ac|}$ which vanishes at both of the boundaries. For infinitesimal δ, the logarithm and arctangent in $I^n_{\ell\Delta}(r^2_\parallel)$ behave as $\log\left|\frac{a-c-\delta}{a-c+\delta}\right| = \frac{2}{c-a}\delta + \mathcal{O}(\delta^3)$ and $\arctan\{(b\pm 2a)/\delta\} = \frac{\pi}{2}\cdot\mathrm{sgn}(b\pm 2a) - \frac{1}{b\pm 2a}\delta + \mathcal{O}(\delta^3)$, respectively. Thus, the limiting behavior of $I^n_{\ell\Delta}(r^2_\parallel)$ is represented as

$$\lim_{r^2_\parallel \to s_-, s_+} I^n_{\ell\Delta}(r^2_\parallel) = \begin{cases} \frac{2}{c-a} + \mathcal{O}(\delta^2) & (r^2_\parallel \to s_- - 0) \\ \{\mathrm{sgn}(b+2a) - \mathrm{sgn}(b-2a)\}\,\pi\delta^{-1} & \\ \quad + \frac{2}{c-a} + \mathcal{O}(\delta^2) & (r^2_\parallel \to s_- + 0 \text{ and } s_+ - 0) \\ 2\pi i\delta^{-1} + \frac{2}{c-a} + \mathcal{O}(\delta^2) & (r^2_\parallel \to s_+ + 0) \end{cases} \tag{H1}$$

where we have used $b^2 \to 4ac$ ($\delta \to 0$) to obtain the zeroth-order term in the middle regime. Note that a negative-power term in the middle regime exists depending on a relative sign between the factors $b \pm 2a$. In Appendix G, we have already examined those signs just above Eq. (G3) and in Eqs. (G4) and (G5). They have the same signs as $b+2a < 0$ and $b-2a < 0$ in the vicinity of the lower boundary $r^2_\parallel = s_- \pm 0$, while the opposite signs as $b + 2a > 0$ and $b - 2a < 0$ in the vicinity of the higher boundary $r^2_\parallel = s_+ \pm 0$. [17] Therefore, $I^n_{\ell\Delta}(r^2_\parallel)$ is finite in the limit $r^2_\parallel \to s_- + 0$, and, on the other hand, $I^n_{\ell\Delta}(r^2_\parallel)$ is divergent in the limit $r^2_\parallel \to s_+ - 0$.

The limiting behaviors of $I^n_{\ell\Delta}(r^2_\parallel)$ are summarized as follows. At $r^2_\parallel = s_-$, it is continuous, and thus has a limiting value $I^n_{\ell\Delta}(r^2_\parallel \to s_-) = 2/(c-a)|_{r^2_\parallel = s_-}$. On the other hand, $I^n_{\ell\Delta}(r^2_\parallel)$ diverges to the positive infinity in the limit $r^2_\parallel \to s_+ - 0$. The real part of $I^n_{\ell\Delta}(r^2_\parallel)$ has a limiting value $I^n_{\ell\Delta}(r^2_\parallel \to s_+ + 0) = 2/(c-a)|_{r^2_\parallel = s_+}$ in the limit $r^2_\parallel \to s_+ + 0$, while the imaginary part diverges to the positive infinity in this limit.

---

[1] W. Heisenberg and H. Euler, Z. Phys. **98** (1936) 714-732, (English translation is available from `arXiv:physics/0605038`).

[17] Remind that the inequality in Eq. (G4) does not contain an equality, and has shown including at the boundary $r^2_\parallel = s_-$. Noting that the factor $b + 2a$ is regular with respect to $r^2_\parallel$ at the boundary, we find that it has the same sign on the both sides of the boundary as far as its infinitesimal vicinity is concerned. The same is true for the other inequality in Eq. (G5) in the infinitesimal vicinity of the boundary $r^2_\parallel = s_+$.

[2] G. V. Dunne, "*Heisenberg-Euler Effective Lagrangians : Basics and Extensions*", (arXiv:hep-th/0406216) published in "*From Fields to Strings: Circumnavigating Theoretical Physics Vol. 1*" (World Scientific, 2005).

[3] V. Weisskopf. The electrodynamics of the vacuum based on the quantum theory of the electron - Kong. Dokl. Akad. Nauk Ser. Fiz. Vid. Selsk. Math-fys. Medd. XIV No. 6 (1936); English translation in "Early Quantum. Electrodynamics: A Source Book", A. I. Miller. (Cambridge University Press, 1994).

[4] K. Itakura, et al. (eds) "Proceedings of International Conference on Physics in Intense Fields (PIF2010)," 24-26 November 2010, KEK, Tsukuba, Japan, available from http://ccdb5fs.kek.jp/tiff/2010/1025/1025013.pdf

[5] D. E. Kharzeev, L. D. McLerran, and H. J. Warringa, Nucl. Phys. A **803** (2008) 227-253.

[6] V. Skokov, A. Y. Illarionov and V. Toneev, Int. J. Mod. Phys. A **24** (2009) 5925-5932; A. Bzdak and V. Skokov, "*Event-by-event fluctuations of magnetic and electric fields in heavy ion collisions*", arXiv:hep-ph/1111.1949.

[7] W. T. Deng and X. G. Huang, Phys. Rev. C **85** (2012) 044907.

[8] K. Itakura, "*Strong Field Physics in High-Energy Heavy-Ion Collisions*", proceedings in [4].

[9] C. Thompson and R. C. Duncan, Mon. Not. Roy. Astron. Soc. **275** (1995) 255, *ibid.* Astrophys. J. **473** (1996) 322.

[10] A. K. Harding and D. Lai, Rept. Prog. Phys. **69** (2006) 2631 [astro-ph/0606674].

[11] K. Tuchin, Phys. Rev. C **82** (2010) 034904 [arXiv:1006.3051 [nucl-th]], *ibid.* Phys. Rev. C **83** (2011) 017901 [arXiv:1008.1604 [nucl-th]], *ibid.* "*Electromagnetic radiation by quark-gluon plasma in magnetic field*," arXiv:1206.0485 [hep-ph].

[12] K. Itakura and K. Hattori, "*Effects of extremely strong magnetic field on photon HBT interferometry*", nucl-th/1206.3022.

[13] Euro. Phys. J. D, Volume 55, Number 2 / November 2009 "*Topical issue on Fundamental physics and ultra-high laser fields*".

[14] W. Tsai, Phys. Rev. D **10** (1974) 2699.

[15] L. F. Urrutia, Phys. Rev. D **17** (1978) 1977.

[16] S. L. Adler, Ann. Phys. **67** (1971) 599-647.

[17] W. Tsai and T. Erber, Phys. Rev. D **10** (1974) 492; *ibid.*, Phys. Rev. D **12** (1975) 1132.

[18] K. Kohri and S. Yamada, Phys. Rev. D **65** (2002), 043006.

[19] D. Melrose and R. Stoneham, Nuovo Cimento A **32** (1976), 435

[20] W. Dittrich and M. Reuter, Lect. Notes Phys. **220** (1985) 1-244.

[21] W. Dittrich and H. Gies, Springer Tracts Mod. Phys. **166** (2000) 1-241.

[22] K. Hattori and K. Itakura, "*Vacuum birefringence in strong magnetic fields: (II) Complex refractive index in the lowest Landau level approximation*", in preparation.

[23] We consistently obey conventions employed in Peskin and Schröder, "*An Introduction To Quantum Field Theory*," (Westview Press, 1995).

[24] J. S. Schwinger, Phys. Rev. **82** (1951) 664-679.

[25] A. E. Shabad, Ann. Phys. **90** (1975) 166-195.

[26] V. N. Baier and V. M. Katkov, Phys. Rev. D **75** (2007) 073009.

[27] A. Erdélyi (ed), Sec. 10.12 in *Higher transcendental functions*, McGraw-Hill, (1953).

[28] A. Chodos, K. Everding and D. Owen, Phys. Rev. D **42** (1990) 2881.

[29] V. P. Gusynin, V. A. Miransky, I. A. Shovkovy, Nucl. Phys. B **462** (1996) 249-290.

[30] K. Fukushima, Phys. Rev. D **83** (2011) 111501.

[31] S. L. Adler, et al., Phys. Rev. Lett. **25** (1970) 1061-1065.

[32] M. G. Baring, "Photon Splitting and Pair Conversion in Strong Magnetic Fields," AIP Conf. Proc. **1051** (2008) 53 [arXiv:0804.0832 [astro-ph]].

[33] M. Abramowitz and I. Stegun, *Handbook of Mathematical Functions*, Dover, New York, (1965).